

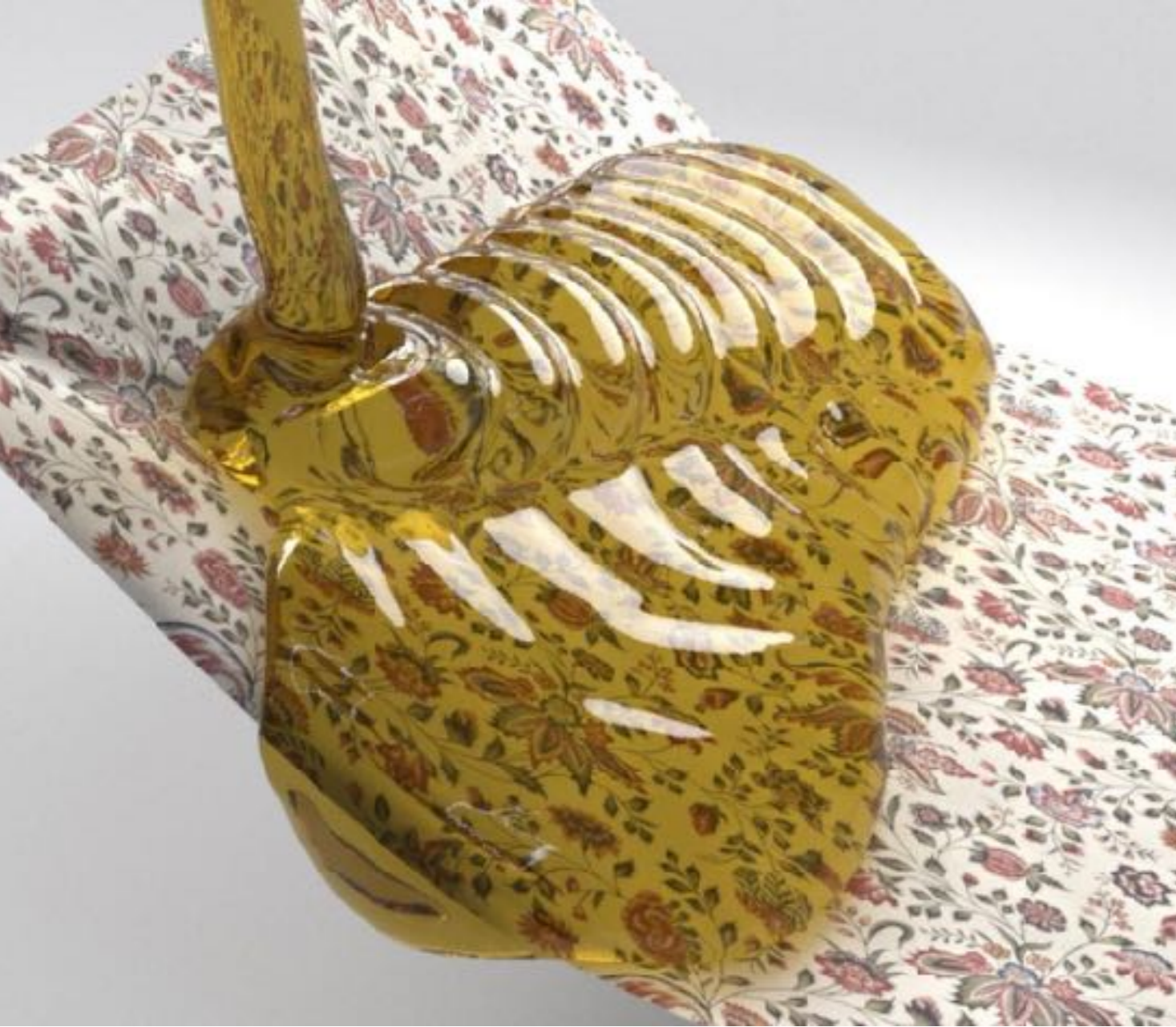
Simulation Methods for Multiphysics Phenomena in Visual Computing

Fabian Löschner, Stefan Rhys Jeske, José Antonio Fernández-Fernández, Jan Bender

Computer Animation Group, RWTH Aachen University



RWTHAACHEN
UNIVERSITY



Part II

Energy-based Multiphysics Models

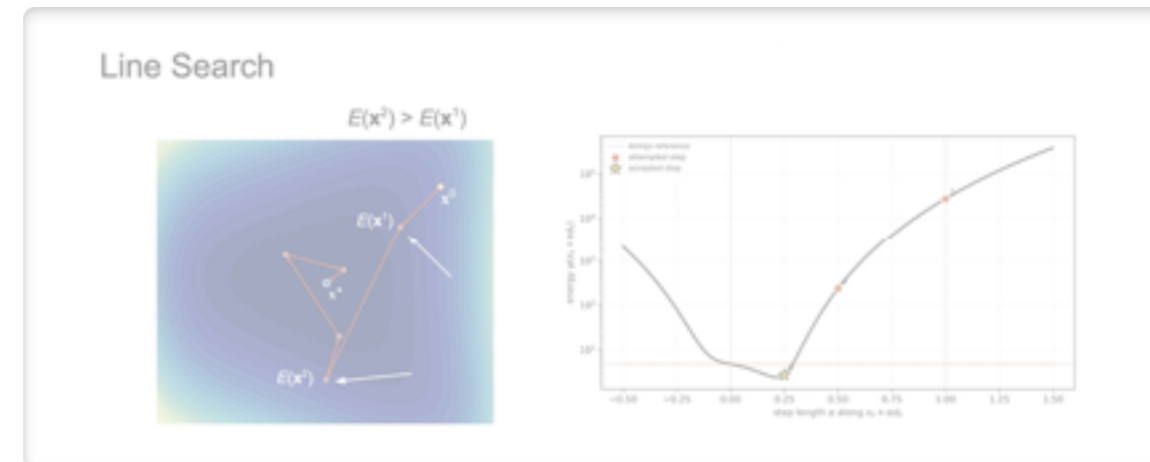
Fabian Löschner, Stefan Rhys Jeske, José Antonio Fernández-Fernández, Jan Bender

Computer Animation Group, RWTH Aachen University



RWTHAACHEN
UNIVERSITY

Outline



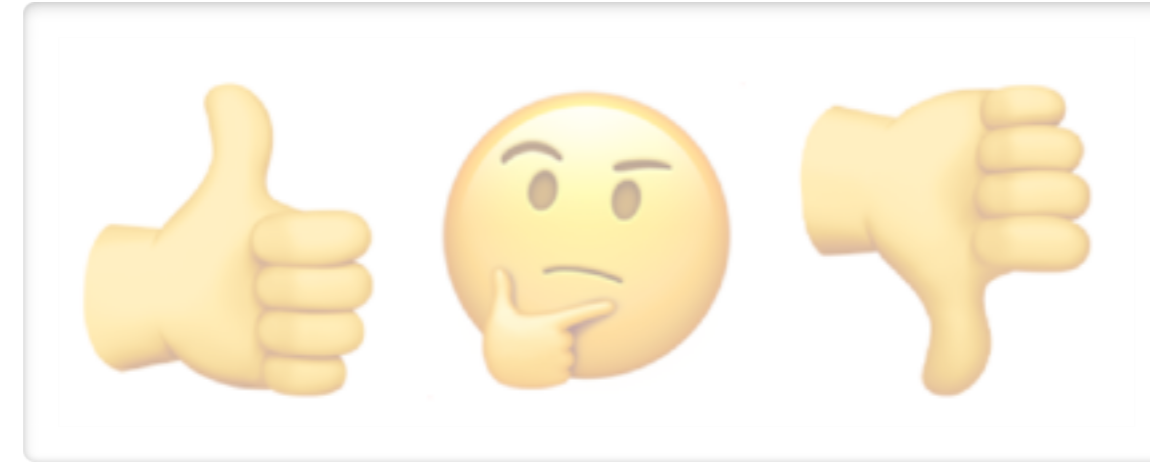
1. Mathematical foundations



2. Physical models and coupling



3. Related methods (VBD, PD)



4. Summary: Models & Properties

Elastic Energies in Computer Graphics

Deformable Solids

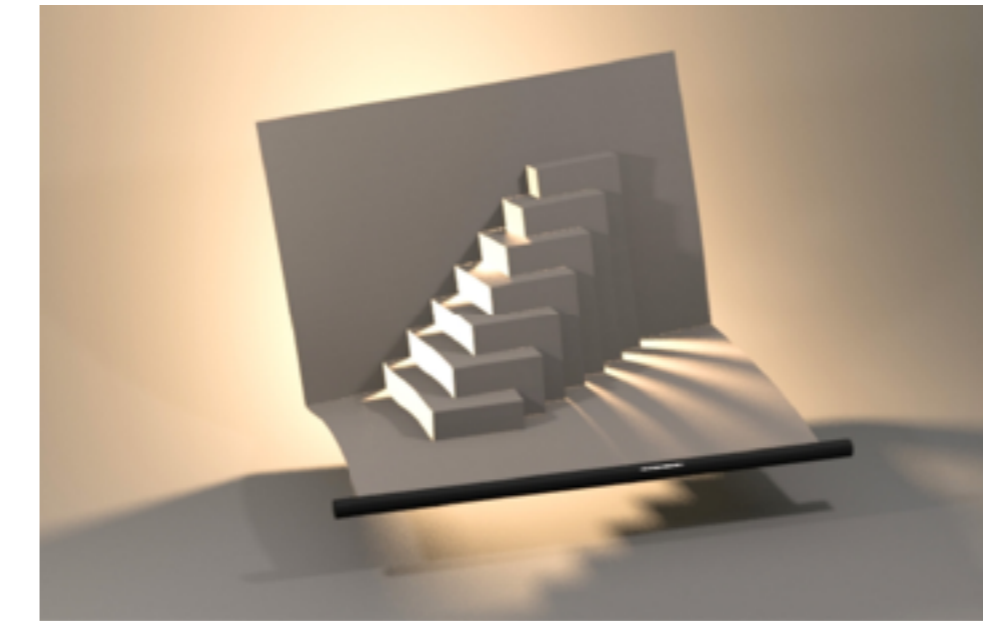


Dynamic Deformables [Kim, Eberle 2022]

Cloth & Shells

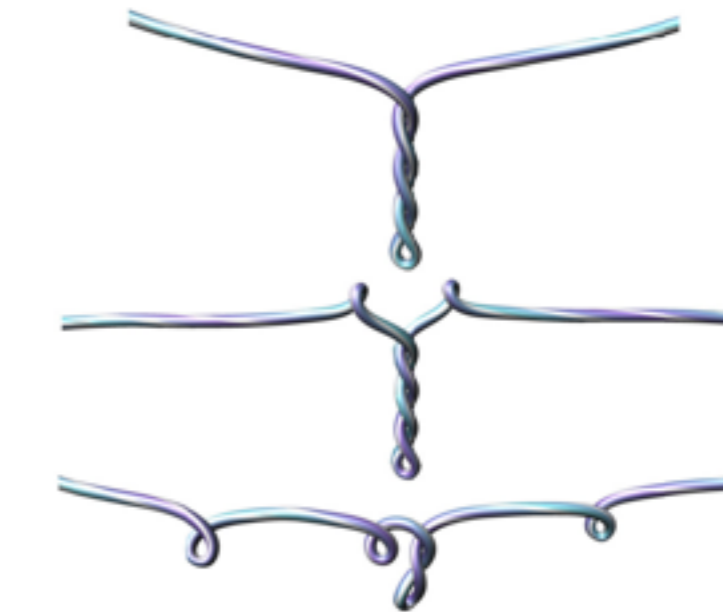


Progressive Dynamics for Cloth and Shell Animation [Zhang et al. 2024]



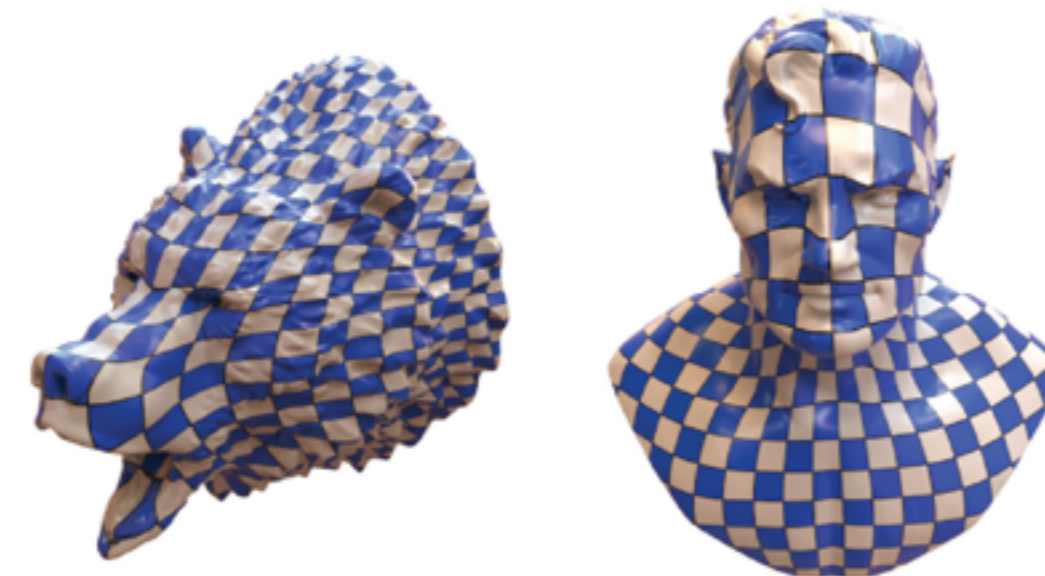
Second-Order Finite Elements for Deformable Surfaces [Le et al. 2023]

Rods



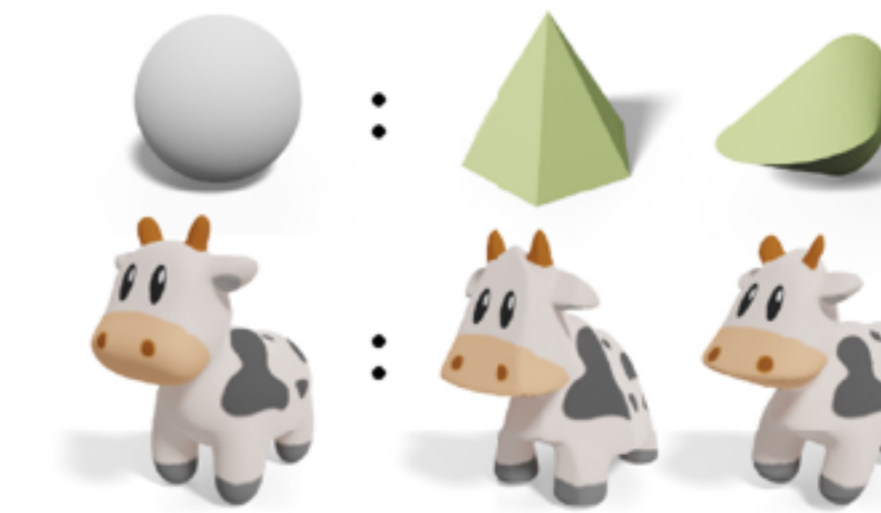
Discrete Elastic Rods [Bergou et al. 2008]

Surface Parametrization



Analytic Eigensystems [Smith et al. 2019]

Shape Stylization & Optimization



Normal-Driven Spherical Shape Analogies [Liu, Jacobson 2021]

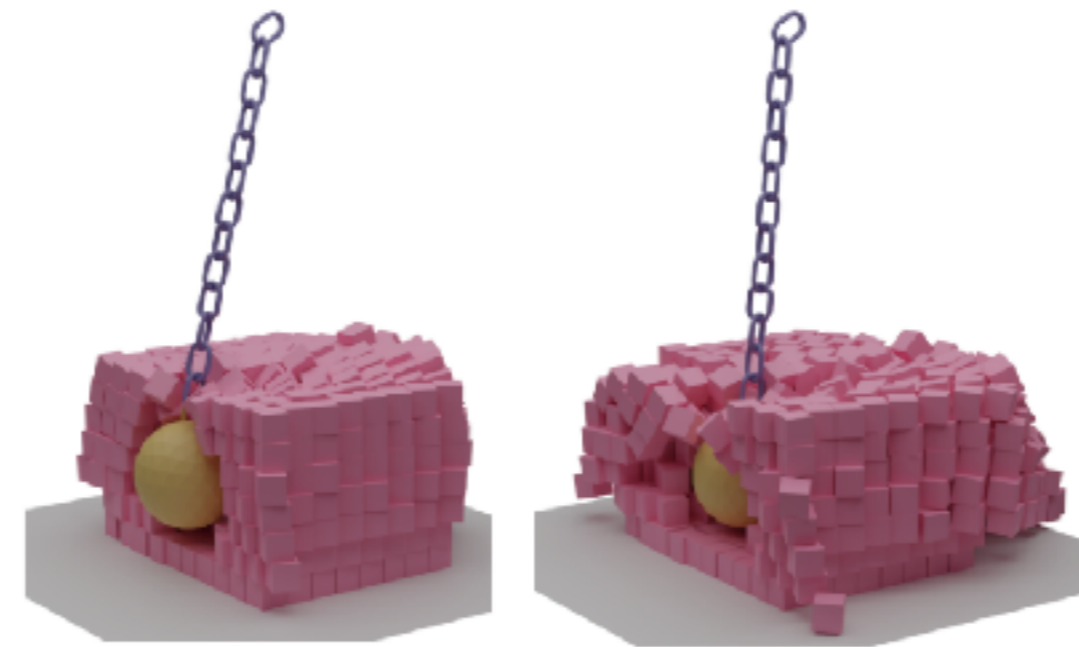
Multiphysics Energies

Contact



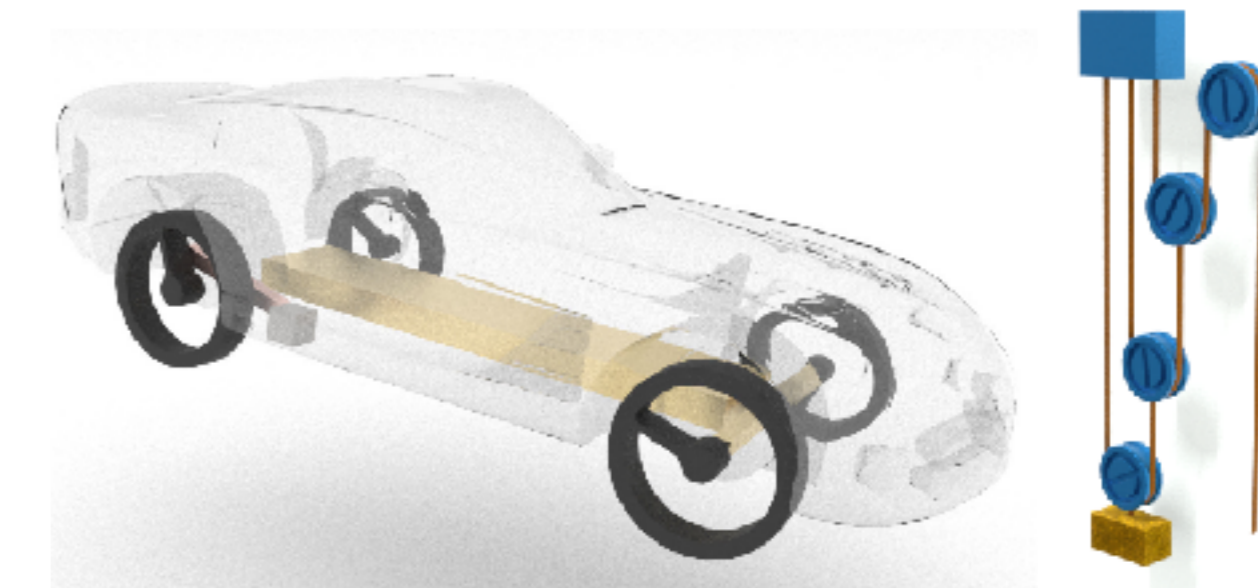
Codimensional Incremental Potential Contact [Li et al. 2021]

Rigid Bodies



Intersection-free Rigid Body Dynamics [Ferguson et al. 2021]

Multibody Systems



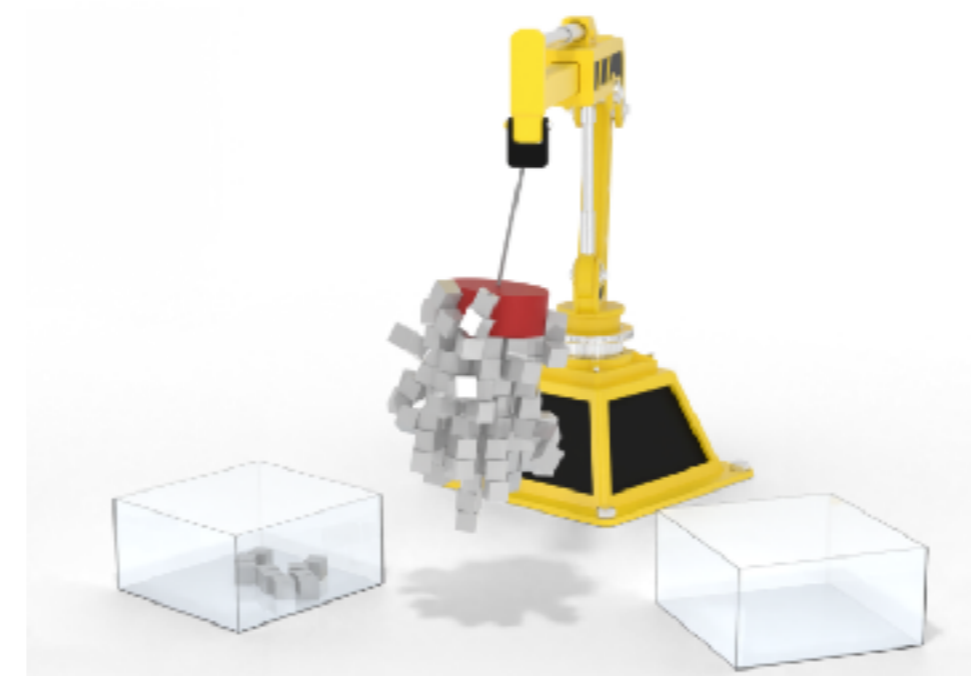
A Unified Newton Barrier Method for Multibody Dynamics [Chen et al. 2022]

Fluids



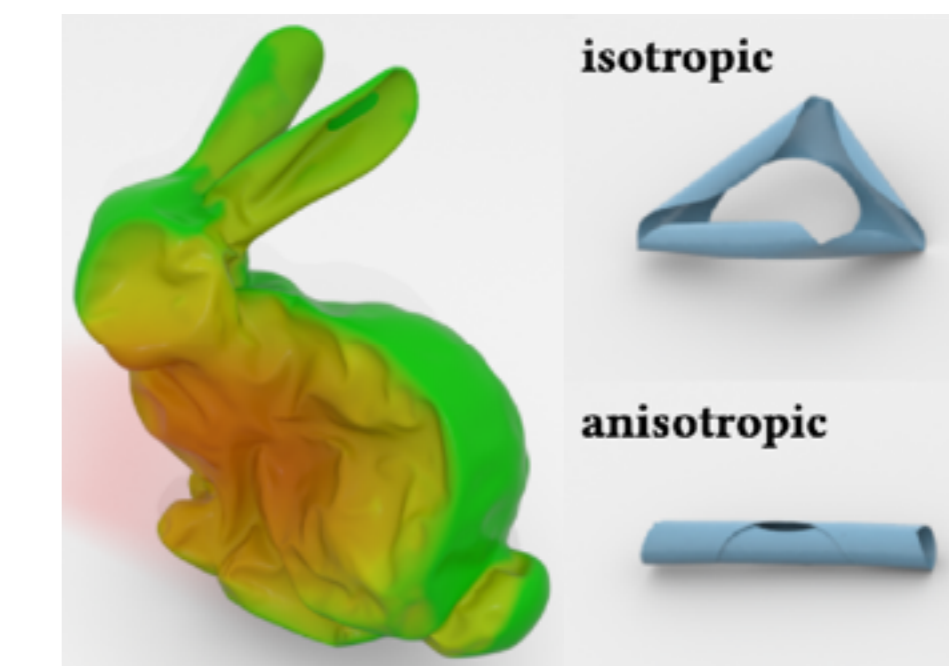
A Contact Proxy Splitting Method for Lagrangian Solid-Fluid Coupling [Xie et al. 2023]

Magnetism



Strongly Coupled Simulation of Magnetic Rigid Bodies [Westhofen et al. 2024]

Heating & Wetting



Physical Simulation of Environmentally Induced Thin Shell Deformation [Chen et al. 2018]

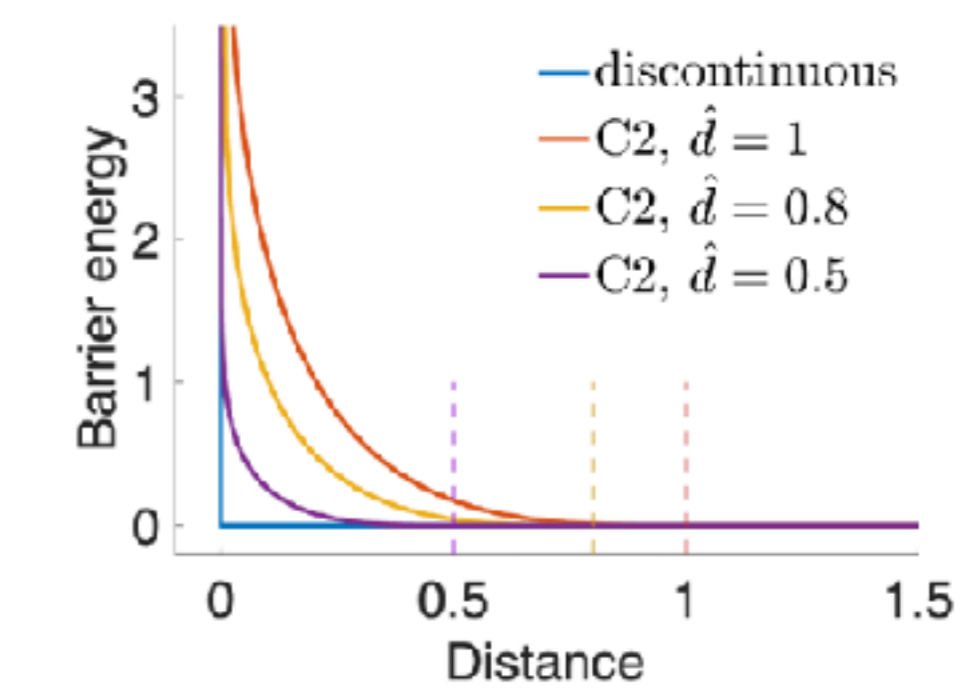
Energy-Based Multiphysics Modeling

Unifying mathematical formulation

- Physical systems modeled by **scalar potentials**
- Constraints modeled by **barrier potentials** or penalties

Typically

- ...leads to fully implicit, **primal** formulation
- ...solved as **unconstrained optimization** problem



Incremental Potential Contact [Li et al. 2020]

Elastic Deformables

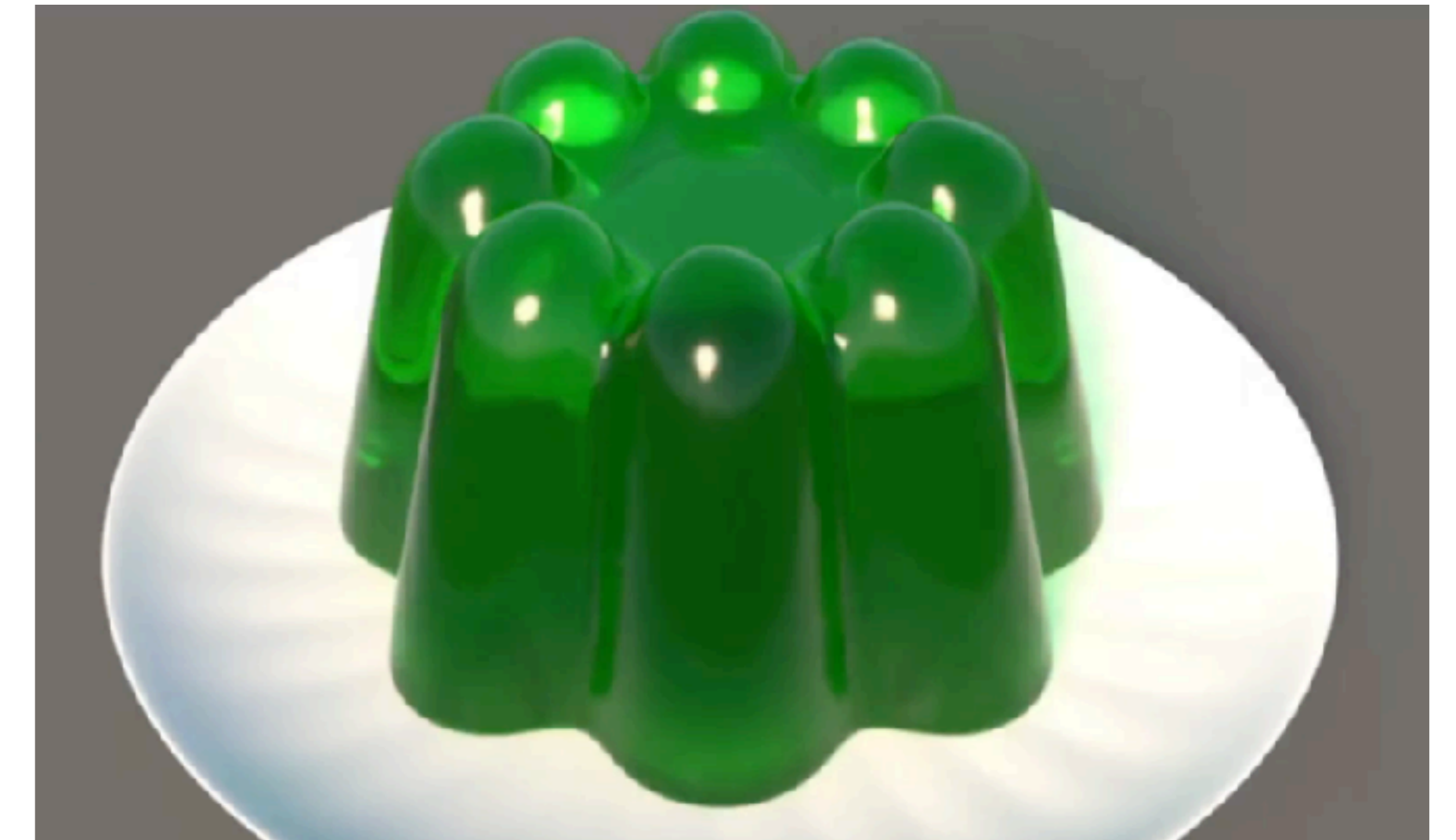
- Naturally described using energies
- Change in shape \rightarrow change in internal energy

- Simple spring-based models

$$\rightarrow \text{e.g. } \phi_{\text{spring}}(\mathbf{x}) = \frac{1}{2}\kappa \left(\|\mathbf{x}_i - \mathbf{x}_j\| - L_0 \right)^2$$

- Continuum-based models: **strain energy densities**

$$\rightarrow \text{e.g. Stable NeoHookean: } \Psi_{\text{SNH}} = \frac{\mu}{2}(\text{tr}(\mathbf{F}^T \mathbf{F}) - 3) - \mu(\det \mathbf{F} - 1) + \frac{\lambda}{2}(\det \mathbf{F} - 1)^2$$



Higher-Order Time Integration for Deformable Solids [Löschner et al. 2020]

Mass Spring Systems

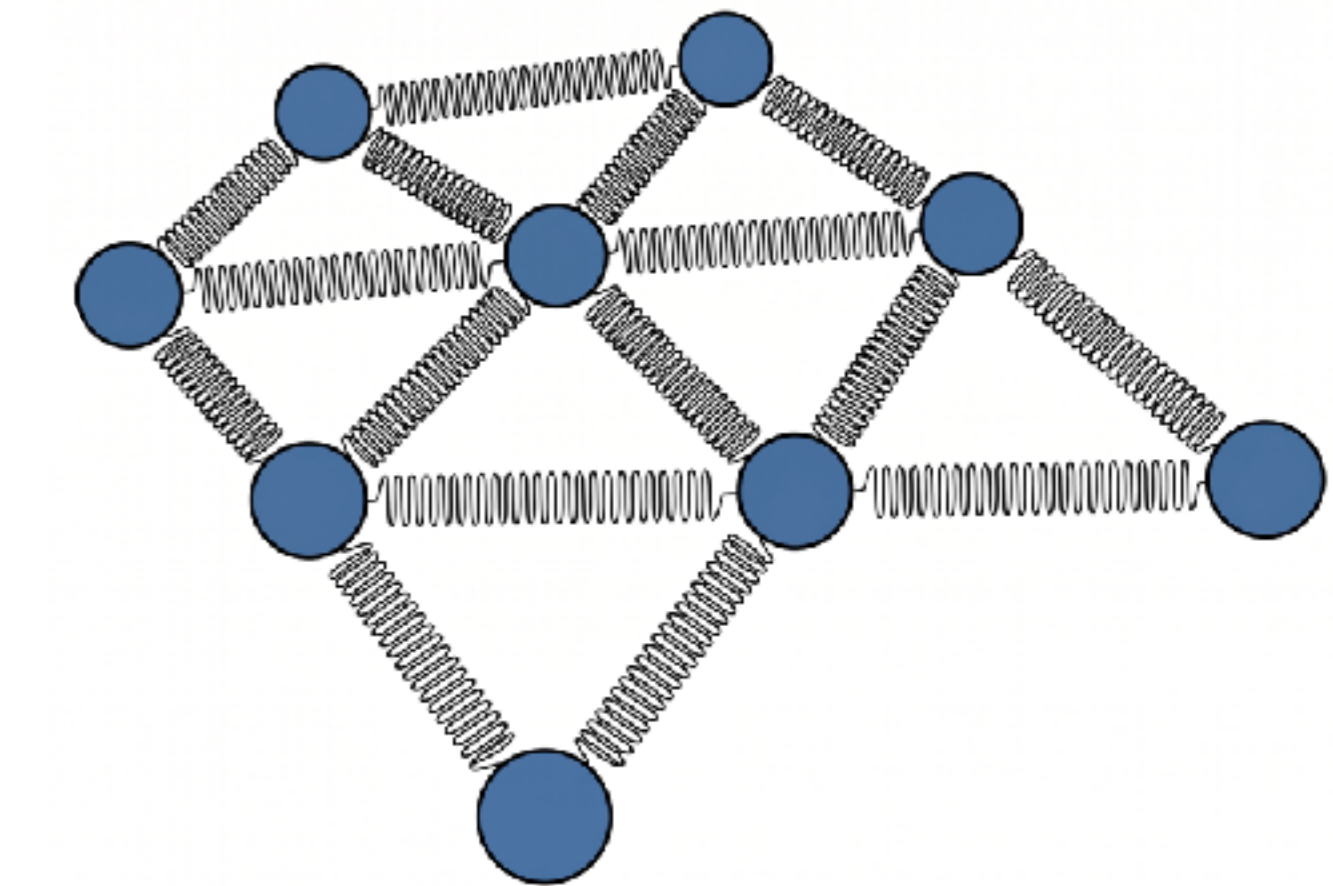
- Needs mesh of geometry (e.g. cloth → tri mesh, solid → tet mesh)
 - Vertices $i \in \mathcal{V}$ become **point masses**: position \mathbf{x}_i and mass m_i
 - Edges $(i, j) \in \mathcal{E}$ become **springs**: stiffness κ_{ij} and rest length L_{ij}
- Energy potential per edge: $\phi_{ij} = \frac{1}{2} \kappa_{ij} (\|\mathbf{x}_i - \mathbf{x}_j\| - L_{ij})^2$

Properties:

- ✓ Easy to implement
- ✓ Extremely fast implementation variants
- ✦ No inherent volume conservation
- ✦ Elastic behavior extremely mesh dependent

Hooke's law:

$$\mathbf{f}_i = -\frac{\partial \phi_{ij}}{\partial \mathbf{x}_i} = -\kappa_{ij} (\|\mathbf{x}_i - \mathbf{x}_j\| - L_{ij}) \frac{\mathbf{x}_i - \mathbf{x}_j}{\|\mathbf{x}_i - \mathbf{x}_j\|}$$



Fast Simulation of Mass-Spring Systems

Tiantian Liu Adam W. Bargteil James F. O'Brien Ladislav Kavan*
 University of Pennsylvania University of Utah University of California, Berkeley University of Pennsylvania

Figure 1: When used to simulate the motion of a cloth sheet with 6561 vertices our method (left) produces real-time results on a single CPU comparable to those obtained with a much slower off-line method (middle). The method also performs well for one-dimensional strands, volumetric objects, and character clothing (right).

Abstract
 We describe a scheme for time integration of mass-spring systems that makes use of a solver based on block coordinate descent. This scheme provides a fast solution for classical linear (Hookean) springs. We express the widely used implicit Euler method as an energy minimization problem and introduce spring directions as

Keywords: Time integration, implicit Euler method, mass-spring systems.

Links: [DL](#) [PDF](#) [VIDEO](#) [W&S](#)

1 Introduction

Kinematic Relations

- Lagrangian description using reference configuration \mathbf{X}
- Displacement field $\mathbf{u}(\mathbf{X}, t)$ gives current configuration $\mathbf{x}(\mathbf{X}, t) = \mathbf{X} + \mathbf{u}(\mathbf{X}, t)$
- Deformation gradient: local linear transformation of material around a point

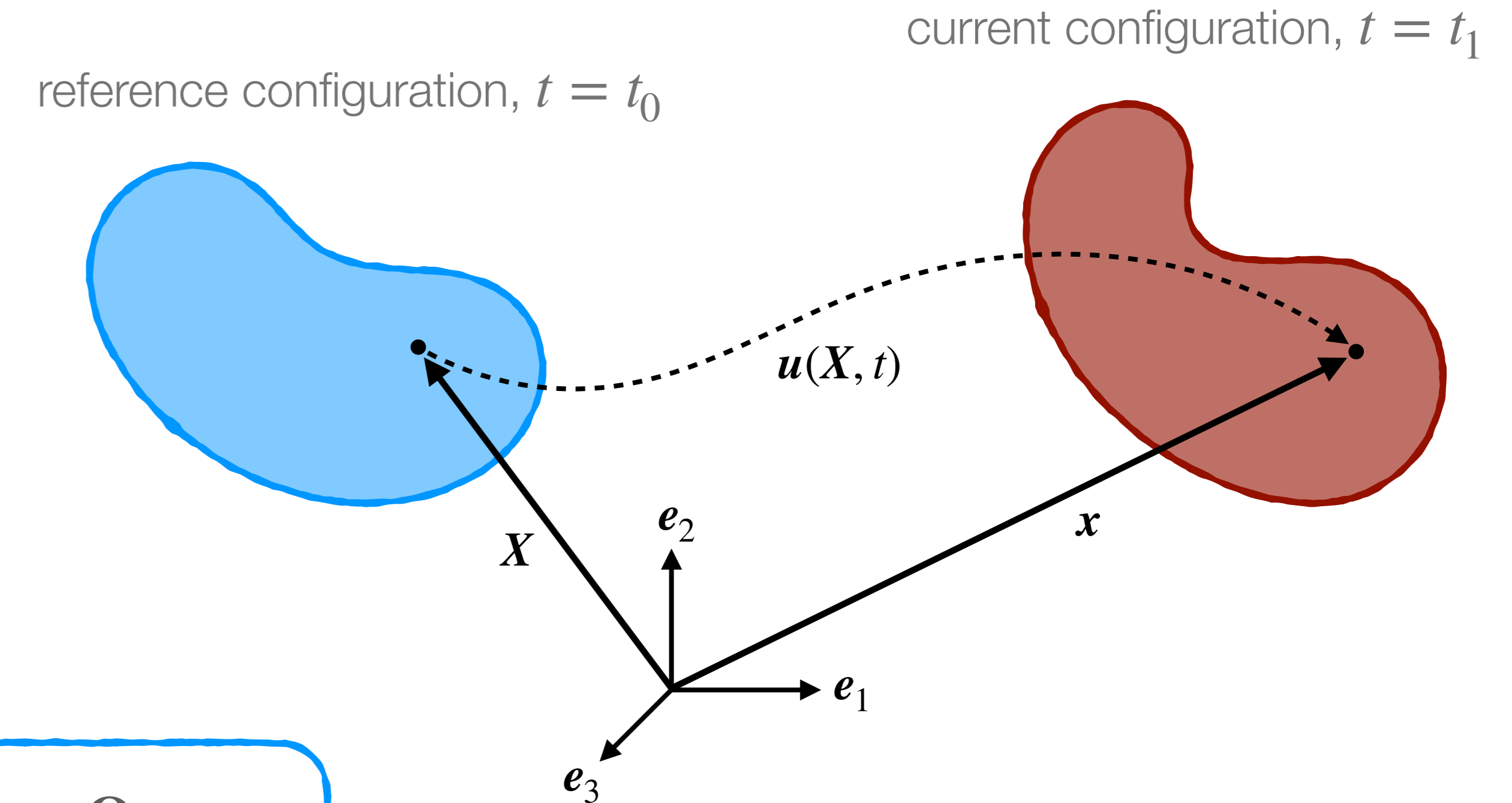
$$\mathbf{F} = \frac{\partial \mathbf{x}}{\partial \mathbf{X}} = \nabla \mathbf{u} + \mathbb{1}$$

Encodes transformation, not just deformation:

- Stretching 👍
- Shearing 👍
- Rotation (and reflection) 🙅

Set $\tilde{\mathbf{x}}(\mathbf{X}) := \mathbf{Q}\mathbf{x}(\mathbf{X})$, where \mathbf{Q} is a rotation matrix. Then:

$$\tilde{\mathbf{F}} = \frac{\partial \tilde{\mathbf{x}}}{\partial \mathbf{X}} = \frac{\partial (\mathbf{Q}\mathbf{x})}{\partial \mathbf{X}} = \mathbf{Q} \frac{\partial \mathbf{x}}{\partial \mathbf{X}} = \mathbf{Q}\mathbf{F}$$

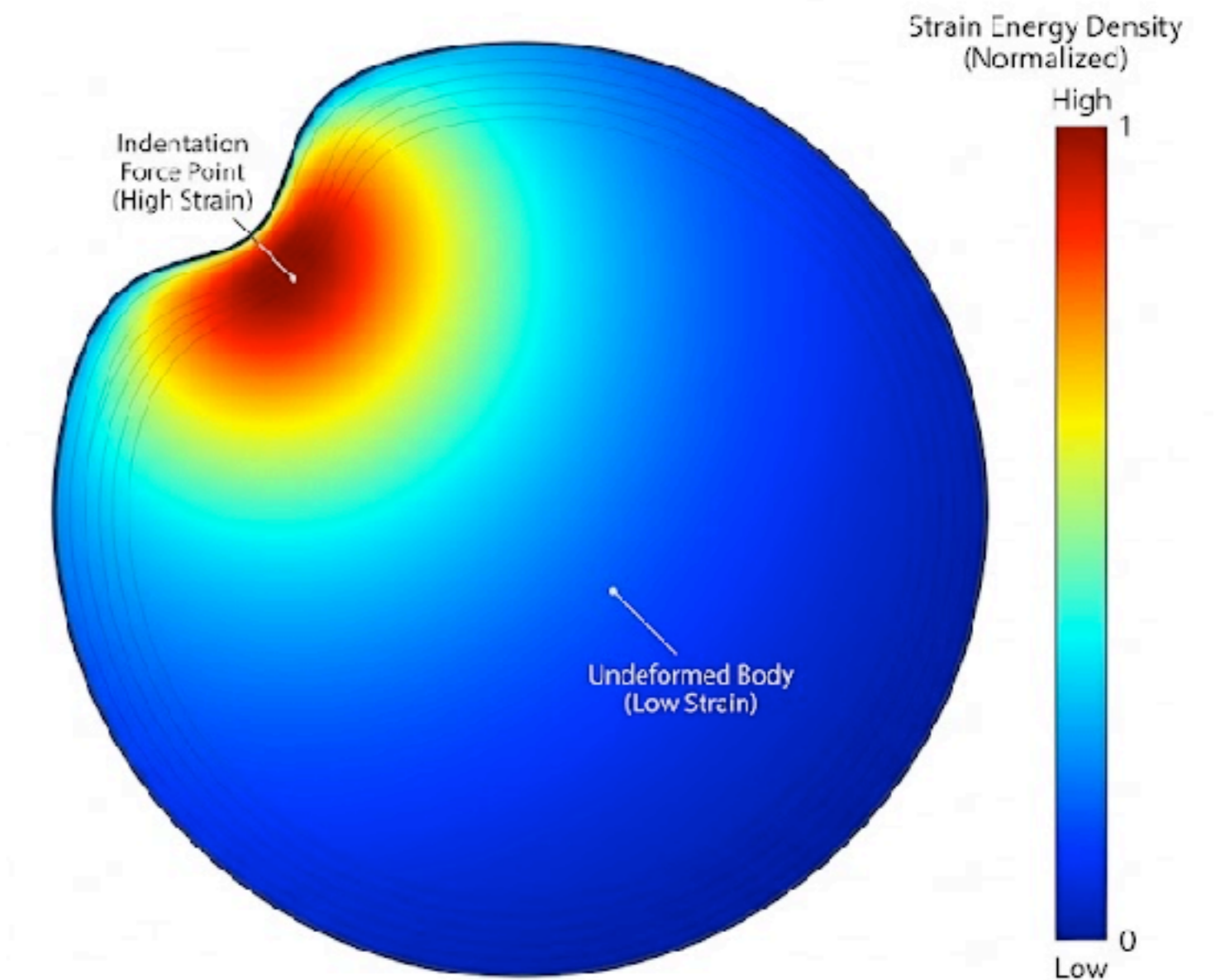


Constitutive Models

- Material defined by scalar **strain energy density** $\Psi(\mathbf{F})$ at every point
- Simplest classic material: **Linear Elasticity**
 - Isotropic generalization of Hooke's Law

$$\Psi_{\text{lin}}(\boldsymbol{\epsilon}) = \underbrace{\frac{\lambda}{2} \text{tr}(\boldsymbol{\epsilon})^2}_{\text{volume conservation}} + \underbrace{\mu \boldsymbol{\epsilon} : \boldsymbol{\epsilon}}_{\text{shape change}} \quad \text{with infinitesimal strain tensor } \boldsymbol{\epsilon} = \frac{1}{2} (\mathbf{F} + \mathbf{F}^T) - \mathbf{I}$$

Properties: → **Constant Hessian** 🎉
 → **Artifacts for finite rotations** ✨



Interactive Virtual Materials
 Matthias Müller Markus Gross
 ETH Zürich

Figure 1: The pitbull with its inflated head (left) shows the artifact of linear FEM under large rotational deformations. The correct deformation is shown on the right.

limitations when it comes to the realistic simulation of material behavior, such as elasticity, plasticity, melting, or fracture. Therefore, methods that control the object by physical laws have received increasing attention.
 In the past decades, computational scientists have devised various methods for the simulation of material behavior with a high level of accuracy. The main goal of such simulations has been the authentic reproduction of the real world, whereas interactivity has not been a primary focus.

Nonlinear Constitutive Models

- Using nonlinear strain measure, e.g. Green Strain: $\mathbf{E} = \frac{1}{2}(\mathbf{F}^\top \mathbf{F} - \mathbb{1})$

- e.g. **St. Venant Kirchhoff** model:

$$\Psi_{\text{StVK}} = \frac{\lambda}{2} \text{tr}(\mathbf{E})^2 + \mu \mathbf{E} : \mathbf{E} \quad (\text{Recall: } \Psi_{\text{lin}}(\boldsymbol{\epsilon}) = \frac{\lambda}{2} \text{tr}(\boldsymbol{\epsilon})^2 + \mu \boldsymbol{\epsilon} : \boldsymbol{\epsilon})$$

Polar decomposition:
 $\mathbf{F} = \mathbf{R}\mathbf{S}$

$$\begin{aligned} \mathbf{E} &= \frac{1}{2}((\mathbf{R}\mathbf{S})^\top \mathbf{R}\mathbf{S} - \mathbb{1}) \\ &= \frac{1}{2}(\mathbf{S}^\top \mathbf{R}^\top \mathbf{R}\mathbf{S} - \mathbb{1}) \\ &= \frac{1}{2}(\mathbf{S}^\top \mathbf{S} - \mathbb{1}) \end{aligned}$$

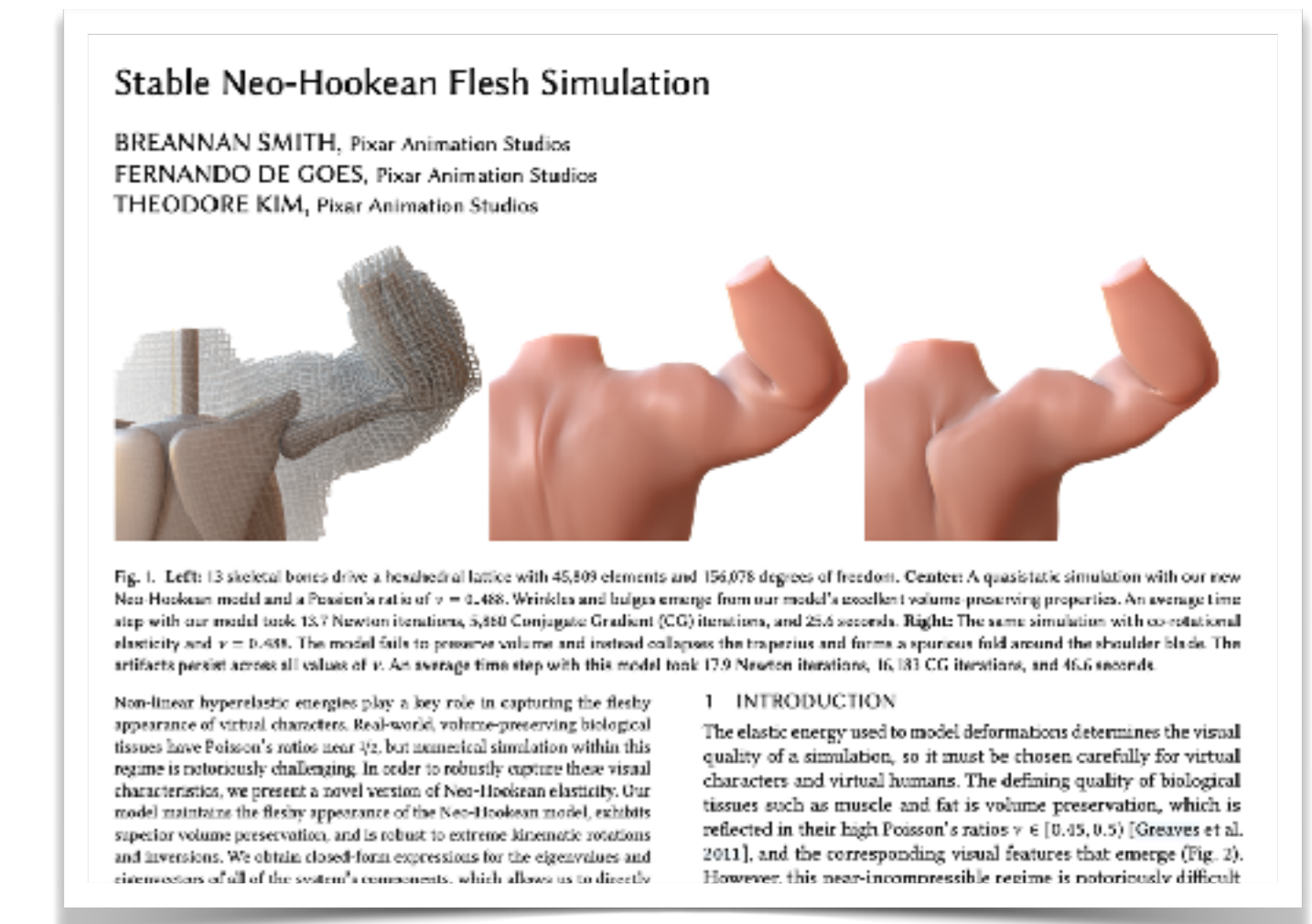
Discards rotation

- Using nonlinear invariants, e.g. from [Smith et al. 2019]: $I_1 = \text{tr}(\mathbf{S})$, $I_2 = \text{tr}(\mathbf{F}^\top \mathbf{F})$, $I_3 = \det \mathbf{F}$

- e.g. **Stable Neo-Hookean** model:

$$\Psi_{\text{SNH}} = \frac{\mu}{2}(I_2 - 3) - \mu(I_3 - 1) + \frac{\lambda}{2}(I_3 - 1)^2$$

- Interpretation: change in energy density due to local length/area/volume changes



Elastic Deformables using FEM

- Continuum-based models: **strain energy densities**

→ e.g. Stable Neo-Hookean: $\Psi_{\text{SNH}} = \frac{\mu}{2}(\text{tr}(\mathbf{F}^T \mathbf{F}) - 3) - \mu(\det \mathbf{F} - 1) + \frac{\lambda}{2}(\det \mathbf{F} - 1)^2$

→ Problem: How to discretize and integrate this?

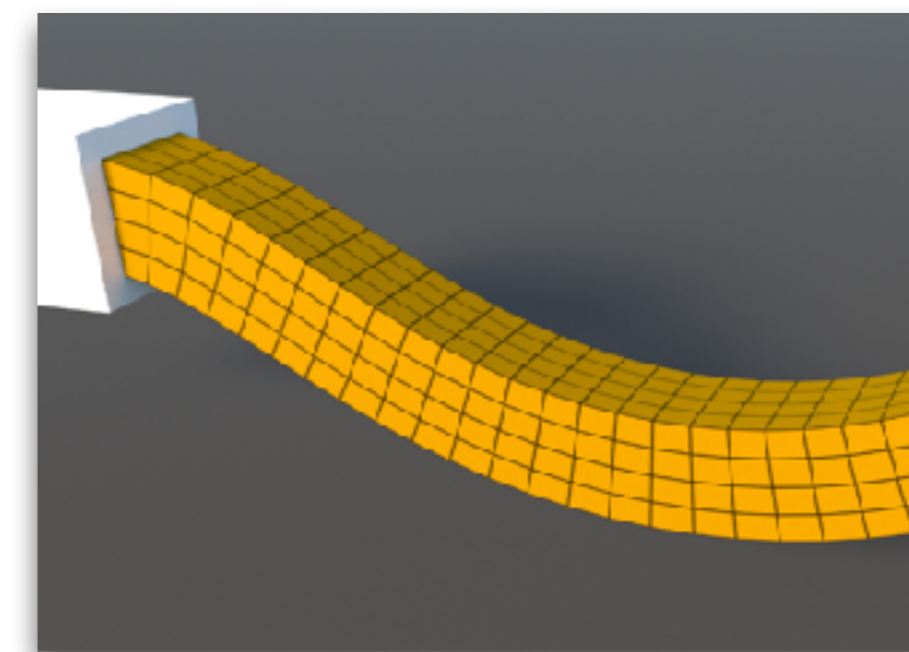
Finite Element Method for discretization

→ Decompose geometry into elements (tetrahedrons, hexahedrons)

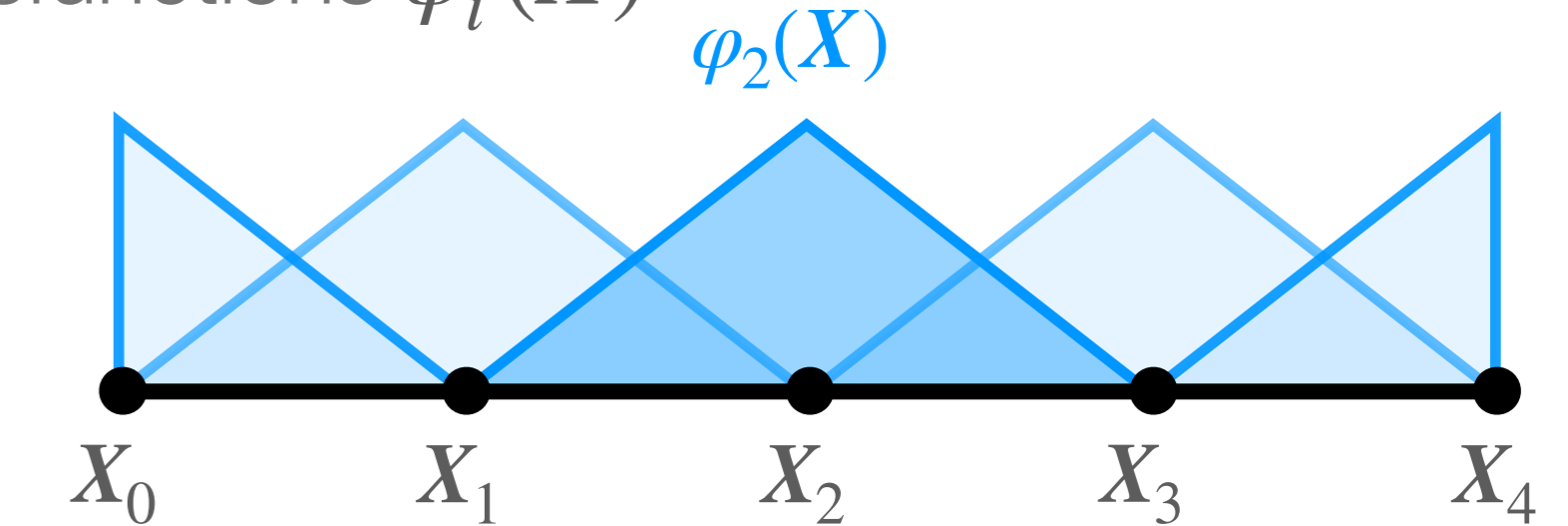
→ Define discrete FEM interpolation of DOF: $\mathbf{u}_h(\mathbf{X}) = \sum_i^N \mathbf{u}_i \varphi_i(\mathbf{X})$

→ Per element: numerical integration of discrete strain energy density

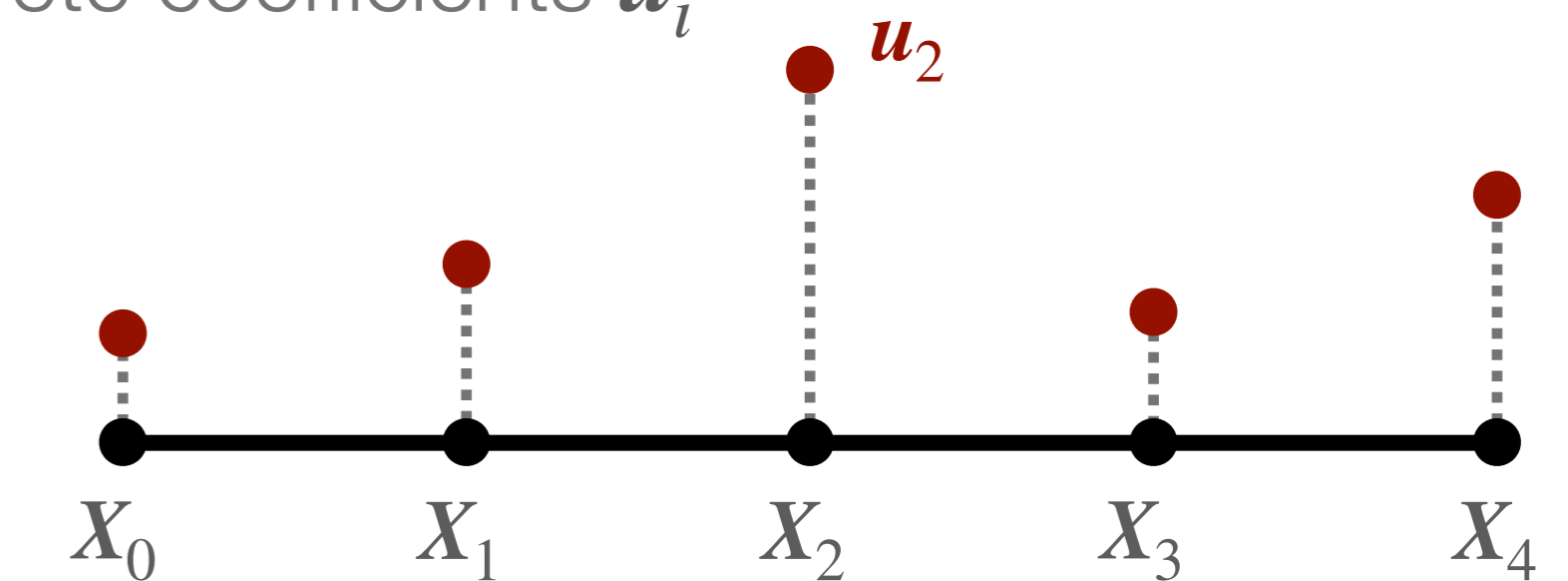
→ Minimize sum of all element energies



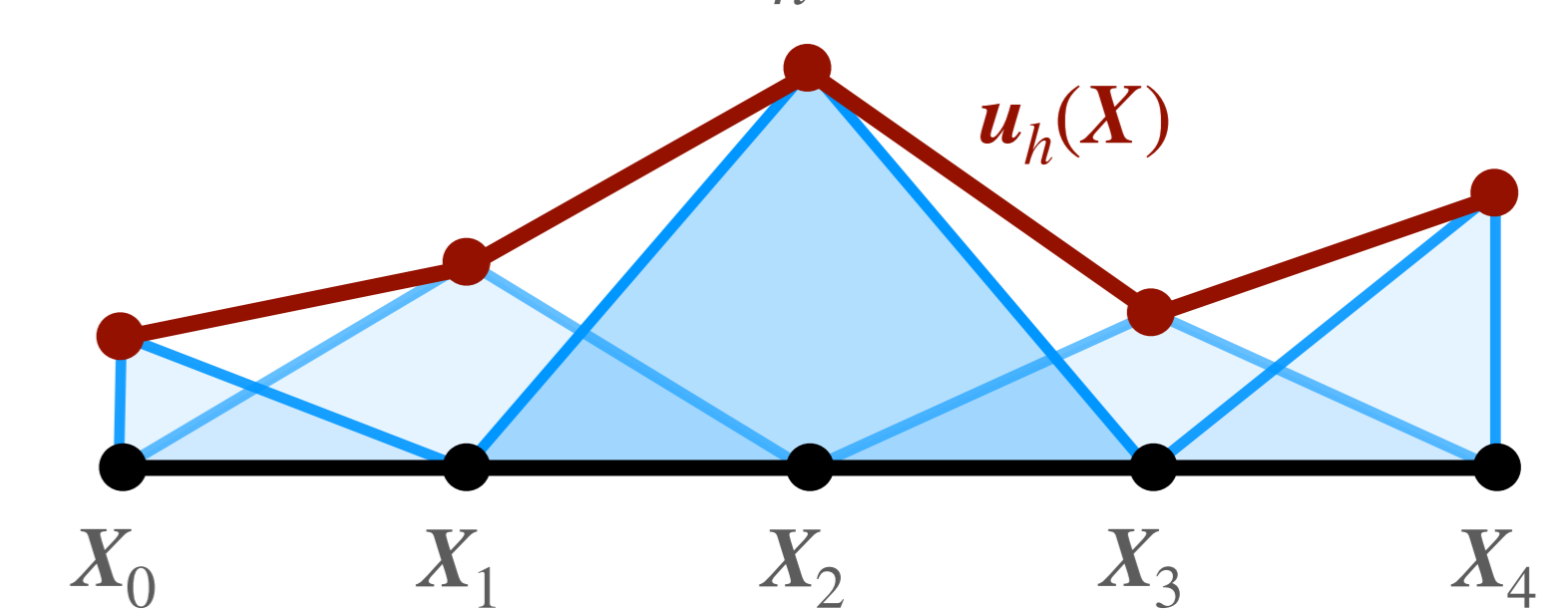
Basisfunctions $\varphi_i(\mathbf{X})$



Discrete coefficients \mathbf{u}_i



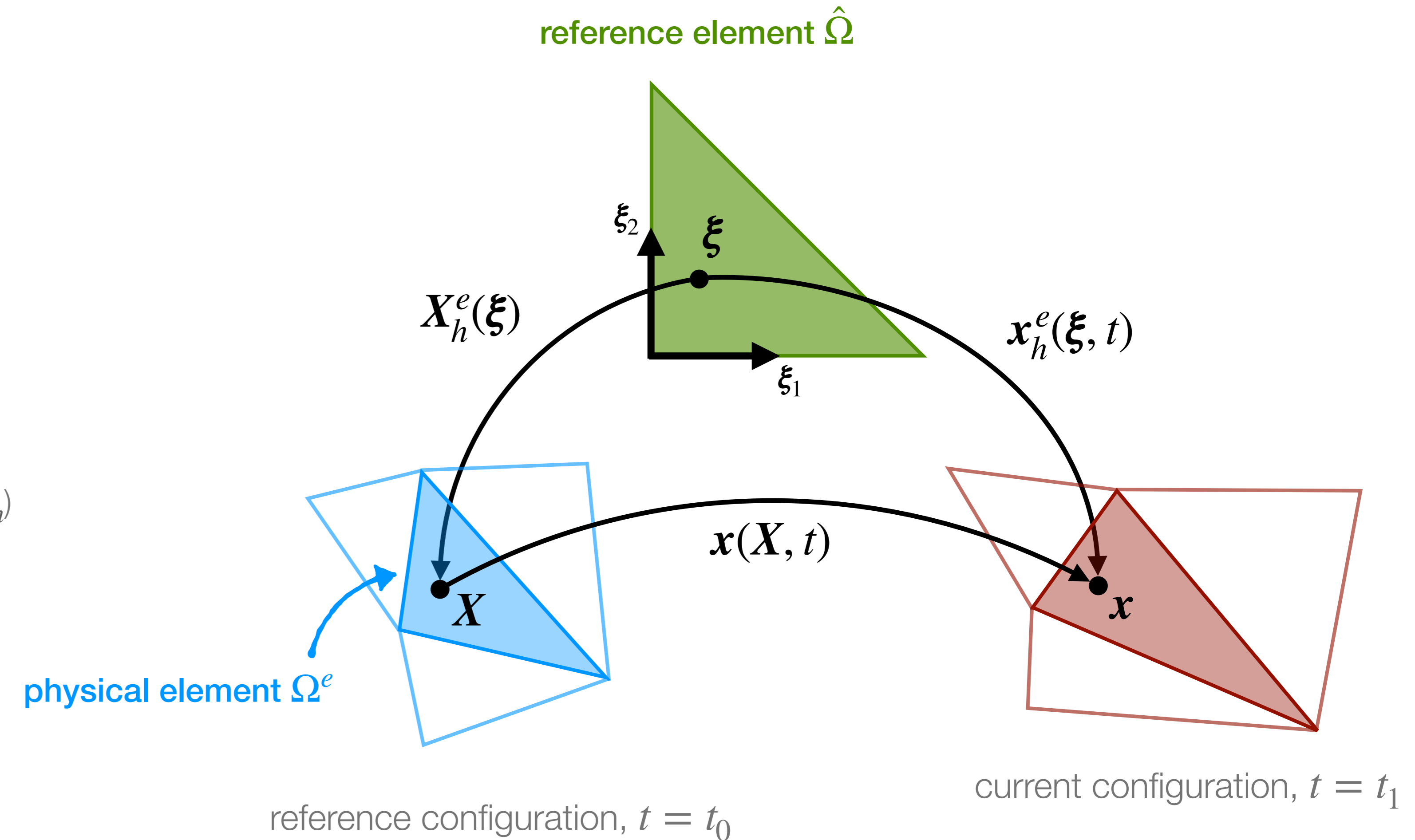
Continuous interpolant $\mathbf{u}_h(\mathbf{X})$



FEM: Evaluating the Strain Energy

- Input: continuous $\Psi(\mathbf{F})$, discrete DOF $\mathbf{u}_i = \mathbf{x}_i - \mathbf{X}_i$
- Goal: numerical integration of strain energy: $\phi^e = \int_{\Omega^e} \Psi(\mathbf{F}) d\mathbf{X}$
 - Would require own quadrature rule per “physical element” Ω^e
- Introduce “reference element” $\hat{\Omega} \subset [0,1] \times [0,1]$ with coordinates $\xi \in \hat{\Omega}$
 - Evaluate quantities and integrals on $\hat{\Omega}$
- **Isoparametric element:** same basis functions for element geometry (\mathbf{X}_h) and unknowns (\mathbf{x}_h or \mathbf{u}_h)
 - Rest coordinates: $\mathbf{X}_h^e(\xi) = \sum_i \mathbf{X}_i^e \hat{\phi}_i(\xi)$
 - Deformed coordinates: $\mathbf{x}_h^e(\xi) = \sum_i \mathbf{x}_i^e \hat{\phi}_i(\xi)$
- Deformation gradient on $\hat{\Omega}$:

$$\mathbf{F}(\xi) = \frac{\partial \mathbf{x}}{\partial \mathbf{X}} = \frac{\partial \mathbf{x}_h^e}{\partial \xi} \frac{\partial \xi}{\partial \mathbf{X}_h^e} = \mathbf{j}^e (\mathbf{J}^e)^{-1}$$



FEM: Evaluating the Strain Energy

- Integrate strain energy density $\Psi(\mathbf{F})$ and transform integral to reference element $\hat{\Omega}$:

$$\phi^e = \int_{\Omega^e} \Psi(\mathbf{F}(\mathbf{X})) d\mathbf{X} = \int_{\hat{\Omega}} \Psi(\mathbf{F}(\boldsymbol{\xi})) \det(\mathbf{J}^e) d\boldsymbol{\xi}$$

- Apply quadrature rule with weights w_i and points $\hat{\mathbf{p}}_i \in \hat{\Omega}$

$$\phi^e \approx \sum_i^{N_{QP}} w_i \Psi(\mathbf{F}(\hat{\mathbf{p}}_i)) \det(\mathbf{J}^e)$$

- In particular, for **linear tetrahedra**:

- Derivatives constant, one quadrature point sufficient

- $\mathbf{J}^e = [\mathbf{X}_1 - \mathbf{X}_0, \mathbf{X}_2 - \mathbf{X}_0, \mathbf{X}_3 - \mathbf{X}_0]$

- $\mathbf{j}^e = [\mathbf{x}_1 - \mathbf{x}_0, \mathbf{x}_2 - \mathbf{x}_0, \mathbf{x}_3 - \mathbf{x}_0]$

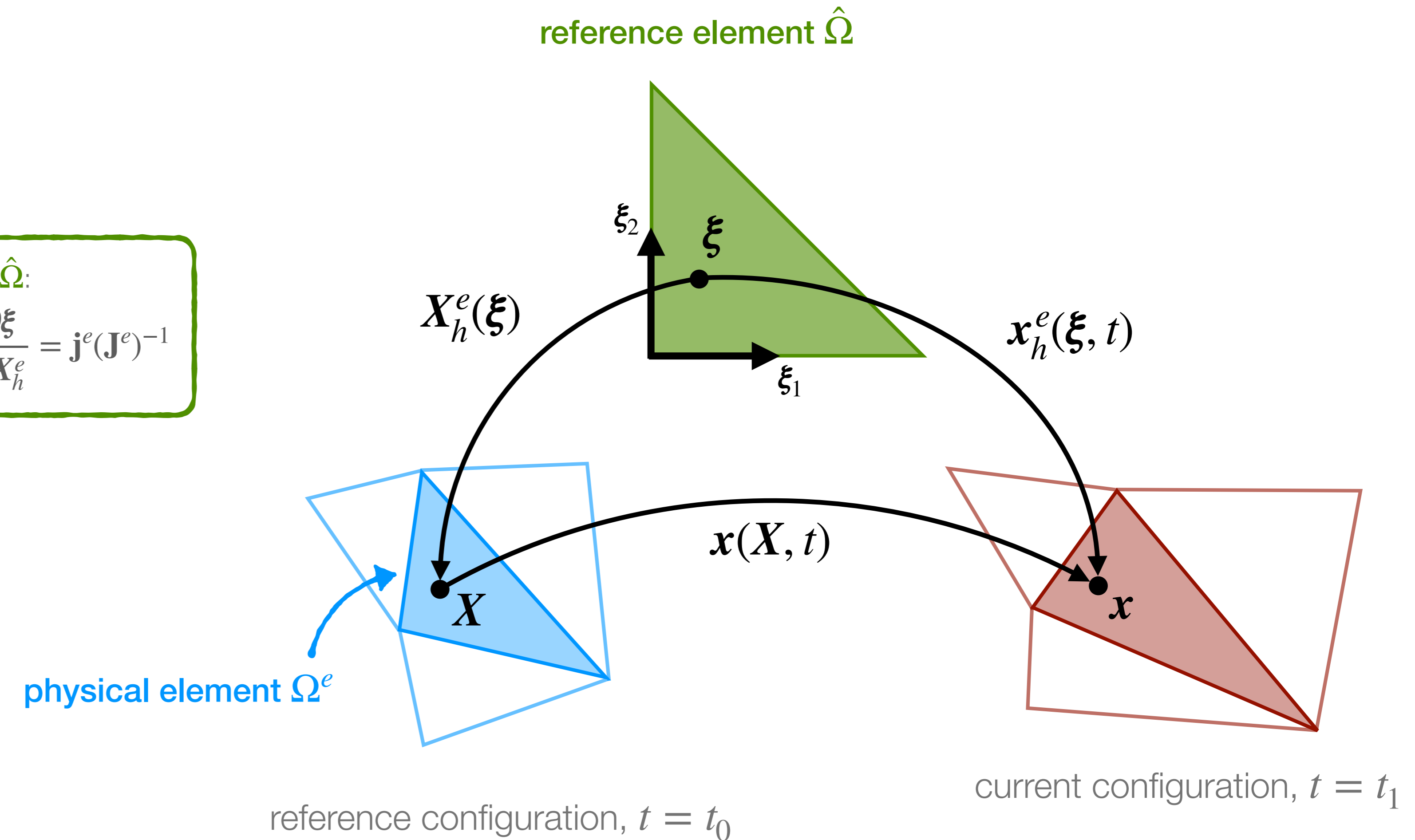
- $\det(\mathbf{J}^e)$ is volume V^e of physical element Ω^e

↳ This yields: $\phi^e = V^e \Psi(\mathbf{j}^e(\mathbf{J}^e)^{-1})$

- Last step: **sum over all elements** and add to incremental potential

Deformation gradient on $\hat{\Omega}$:

$$\mathbf{F}(\boldsymbol{\xi}) = \frac{\partial \mathbf{x}}{\partial \mathbf{X}} = \frac{\partial \mathbf{x}_h^e}{\partial \boldsymbol{\xi}} \frac{\partial \boldsymbol{\xi}}{\partial \mathbf{X}_h^e} = \mathbf{j}^e(\mathbf{J}^e)^{-1}$$



Modelling Dynamic Contact

- Incremental Potential Contact [Li et al. 2020]
 - ↳ Goal: intersection-free simulations in unconstrained optimization
- Introduce smoothly clamped barriers:

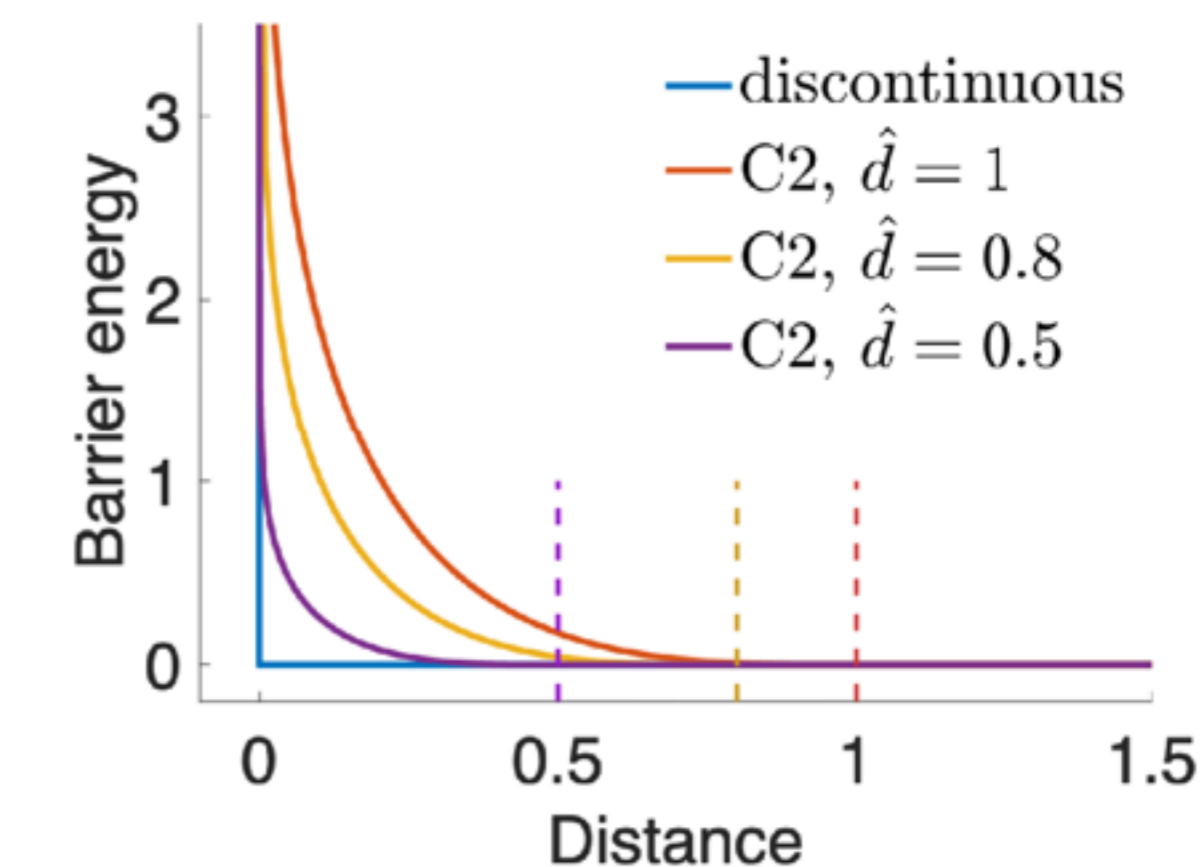
$$b(d, \hat{d}) = \begin{cases} -(d - \hat{d})^2 \ln\left(\frac{d}{\hat{d}}\right), & 0 < d < \hat{d} \\ 0 & d \geq \hat{d} \end{cases}$$

With contact potential $\phi_C(\mathbf{x}) = \kappa \sum_{k \in \mathcal{C}} b(d_k(\mathbf{x}))$

- Apply barriers to all triangle-vertex and edge-edge pairs $k \in \mathcal{C}$
- Filtered line search: CCD determines upper bound for step



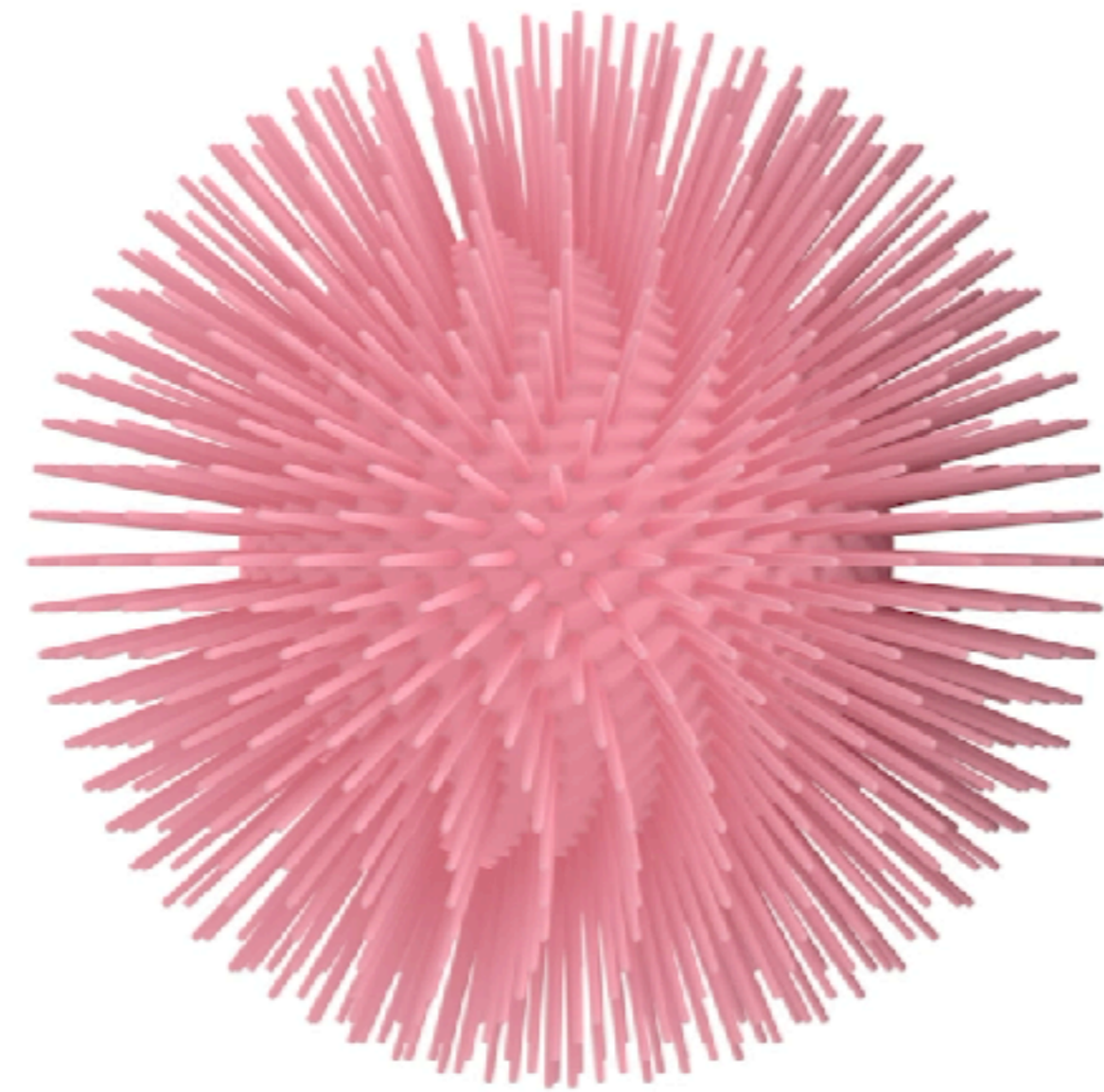
Incremental Potential Contact [Li et al. 2020]



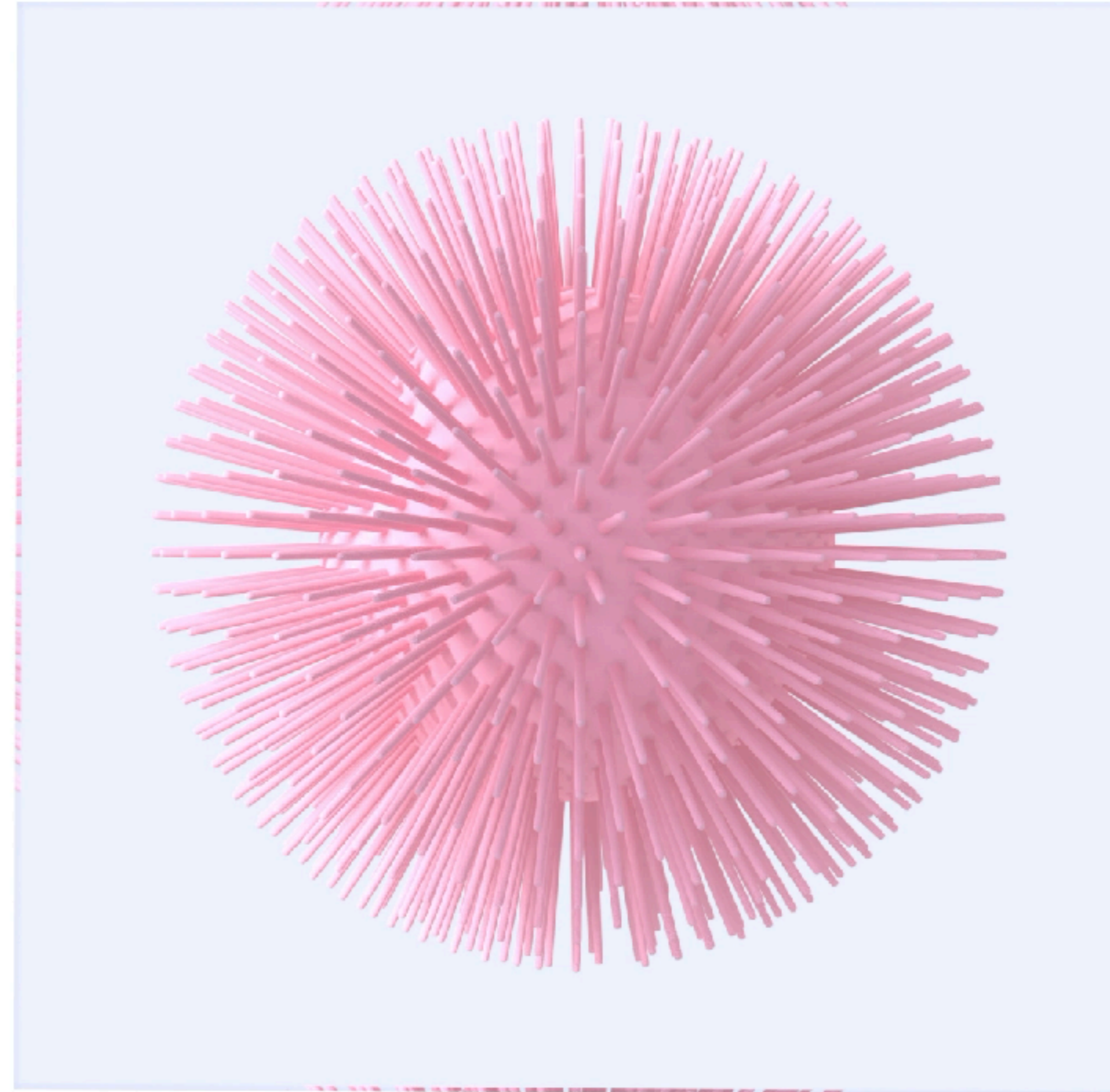
Incremental Potential Contact [Li et al. 2020]

Intersection-free Dynamic Contact

IPC



tetrahedra: 2314K
contacts per step (max): 105K
dt: 0.001
 μ : 0



Incremental Potential Contact [Li et al. 2020]

Intersection-free Dynamic Contact

tetrahedra: 181K
contacts per step (max): 277K
dt: 0.01
 $\mu: 0$



Intersection-free Dynamic Contact

High-Order Incremental Potential Contact for Elastodynamic Simulation on Curved Meshes

Zachary Ferguson
zfergus@nyu.edu
New York University
USA

Pranav Jain
pranav.jain@nyu.edu
New York University
USA

Denis Zorin
dzorin@cs.nyu.edu
New York University
USA

Tesco Schneider
tesen@uvic.ca
University of Victoria
Canada

Daniele Panozzo
panozzo@nyu.edu
New York University
USA

GIPC: Fast and Stable Gauss-Newton Optimization of IPC Barrier Energy

KEMENG HUANG, The University of Hong Kong, TransGP, Hong Kong
FLOYD M. CHITALU, The University of Hong Kong, TransGP, Hong Kong
HUANCHENG LIN, The University of Hong Kong, TransGP, Hong Kong
TAKU KOMURA, The University of Hong Kong, TransGP, Hong Kong

Fig. 1. We offer a robust method enabling simultaneous construction and projection of approximated IPC barrier Hessians to positive semi-definite state for faster implicit time integration. A multilayered cloth animation is shown, where contacts are resolved using our method, which ensures fast convergence rates without numerical eigendecompositions of local barrier Hessians.

A Cubic Barrier with Elasticity-Inclusive Dynamic Stiffness

RYOICHI ANDO, ZOZO, Japan

Fig. 1. Five cylindrical shells are individually twisted and bundled together (A). A single woven cylinder is twisted forming intricate buckles (B). A set of lengthy strands are poured into a bowl (C). Fluttering ribbons are poured into a bowl followed by a strong impact from a falling sphere (D). A fishing knot is tightened (E). Eight squishy hairy balls are compressed and released (F). A house of cards collapses with a gentle touch by a rolling sphere (G). Ten sheets are smashed onto the ground by a fast falling heavy sphere (H). Peak contact counts are 168.33 million (A), 17.59 million (D), 6.49 million (C), 6.04 million (B), 5.63 million (H), 2.89 million (F). Average time per video frame is 194s (A), 745s (B), 247s (C), 184s (D), 3.30s (E), 196s (F), 5.04s (G), 77.35s (H).

This paper presents a new cubic barrier with elasticity-inclusive dynamic stiffness for penetration-free contact resolution and strain limiting. We show that our method enlarges tight strain-limiting gaps where logarithmic purely volumetric approaches ill-suited for codimensional colliders [Allard et al. 2010; Chen et al. 2023; Faure et al. 2008; Tang et al. 2012]. If collisions are unresolvable, one may resort to a rigid impact

Second-order Stencil Descent for Interior-point Hyperelasticity

LEI LAN, The University of Utah, USA
MINCHEN LI, UCLA, USA
CHENFANFU JIANG, UCLA, USA
HUAMIN WANG, Style3D Research, China
YIN YANG, The University of Utah & Style3D Research, USA

Fig. 1. Falling barbarian ships. We propose a new GPU-based algorithm for generic finite element simulation using interior-point methods. Due to the use of barrier functions, interior-point methods are expensive, and the requirement of per-iteration CCD imposes extra challenges for GPU parallelization. Our method is locally second-order leveraging complex-step finite difference to efficiently estimate local Hessian-vector products. We design a complementary coloring and hybrid sweep scheme to fully exploit the throughput of the GPU. Together with a dedicated warm-start process, our method offers speedup of two orders, even with intense contacts and collisions. As a demonstration, the teaser figure shows snapshots of two barbarian ships falling on a spiral stair. There are nearly one million (974K) elements on the ships. The thin paddles at both sides collide with the staircase and the handrails yielding rich and interesting deformations. Under the time step of $\Delta t = 1/100$ sec, our simulation faithfully captures all the details but it is 129x faster than the vanilla CPU

Preconditioned Nonlinear Conjugate Gradient Method for Real-time Interior-point Hyperelasticity

Xing Shen
Fuxi AI Lab, NetEase Inc
Hangzhou, Zhejiang, China
shenxing03@corp.netease.com

Runyuan Cai
Fuxi AI Lab, NetEase Inc
Hangzhou, Zhejiang, China
cairunyuan@corp.netease.com

Mengxiao Bi
Fuxi AI Lab, NetEase Inc
Hangzhou, Zhejiang, China
bimengxiao@corp.netease.com

Tangjie Lv
Fuxi AI Lab, NetEase Inc
Hangzhou, Zhejiang, China
hztvtangjie@corp.netease.com

Figure 1: Example simulation results involving complex self-collision scenarios.

Barrier-Augmented Lagrangian for GPU-based Elastodynamic Contact

DEWEN GUO, Peking University, China
MINCHEN LI, Carnegie Mellon University, United States of America
YIN YANG, University of Utah, United States of America
SHENG LI, Peking University, China
GUOPING WANG, Peking University, China

Fig. 1. Puffer Balls on Nets: Simulations among Heterogeneous Materials. In this scenario, we simulate the interaction of four puffer balls with a chain-net characterized by different Young's moduli: (a) $E = 100$ MPa, and (b) $E = 1$ GPa. All puffer balls are modeled using the Neo-Hookean elasticity model with $E = 5 \times 10^5$ Pa. Despite the use of high resolution meshes with over 1.76 million tetrahedra and a large time step size of 1/30 s, our simulation framework maintains robustness and efficiency. With GPU acceleration implemented, the computation time per frame for scenario (b) is only 427 seconds, without sacrificing accuracy. This represents a notable speedup of 80.1x compared to the IPC [Li et al. 2020], which requires approximately 9.5 hours per frame for the

Cloth, Shells & Rods

Shell models (examples...)

Discrete Shells

Eran Ertugrul¹ Amir N. Hiran¹ Mathieu Desbrun¹ Peter Schröder¹
ETH Zurich Caltech USC Caltech

Abstract: In this paper we introduce a discrete shell model describing the behavior of thin flexible structures such as sails, leaves, and membranes, which are characterized by a curved undeformed configuration. Previously such models required complex variational mechanical formulations and computationally complex simulations. We show that a simple shell model can be derived geometrically for dynamic shells and implemented quickly by modifying a standard cloth simulator. Our technique convincingly simulates a variety of curved objects with materials ranging from paper to metal, as we demonstrate with several examples including a comparison of a real and simulated juggling hat.

Categories and Subject Descriptors (according to ACM CCS): I.3.7 [Computer Graphics]: Three-Dimensional Graphics and Realism—Animation; I.6.R [Simulation and Modeling]: Types of Simulations—Animation.

Second-Order Finite Elements for Deformable Surfaces

Qiqin Le¹ Yitong Deng¹ Jianyu Bu¹
Shanghai Qi Zhi Institute Dartmouth College Tsinghua University
 Shanghai, China Hanover, United States of America Beijing, China
 leqq@qzhi.cn yitong.deng@dartmouth.edu bujy@sem.tsinghua.edu.cn

Bo Zhu¹ Tao Du¹
Georgia Institute of Technology Tsinghua University
 Atlanta, United States of America Beijing, China
 Dartmouth College Shanghai Qi Zhi Institute
 Hanover, United States of America Shanghai, China
 bo.zhu@gatech.edu tao.du@tshinghua.edu.cn

Geometrically motivated

Kirchhoff-Love Shells with Arbitrary Hyperelastic Materials

JIAHAD WEN¹, University of Southern California, USA
 JERNEJ BARBIĆ¹, University of Southern California, USA

Fig. 1. Our technique can simulate Kirchhoff-Love thin shells with arbitrary hyperelastic materials. We show a thin-shell cloth draped against a base in both its rest pose, for three nonlinear materials. The hyperelastic materials include chains of principal stretches in their definitions, and cannot be simulated using prior work. Observe the different folds, and thickness changes, under the three different materials.

Multi-Layer Thick Shells

Curved Three-Director Cosserat Shells with Strong Coupling

F. Lötchen¹, J. A. Fernández-Fernández¹, S. R. Jaska¹ and J. Bender¹
RWTH Aachen University, Germany

Figure 1: Two scenes with curved geometries demonstrate our incremental potential formulation of a Cosserat shell model. It is strongly coupled to other systems through frictional contact based on “High-Order IPC” [23, 27, 28]. Left: An untwisted “sheet of papyrus”

Continuous models

Intersection-free contact

Codimensional Incremental Potential Contact

MINCHEN LI, University of California, Los Angeles, University of Pennsylvania, & Adobe Research
 DANNY M. KAUFMAN, Adobe Research
 CHENFANFU JIANG, University of California, Los Angeles & University of Pennsylvania

Fig. 1. Table cloth pull: (a) accurate, controllable strain laid on a table with heavy, while accurately resolving the pull speed increase at 1m/s, the settling on table with wrinkling behaviors in the

A Cubic Barrier with Elasticity-Inclusive Dynamic Stiffness

RYOICHI ANDO, ZOZO, Japan

Fig. 1. Five cylindrical shells are individually twisted and bundled together (A). A single woven cylinder is twisted forming intricate buckles (B). A set of lengthy strands are poured into a bowl (C). Fluttering ribbons are poured into a bowl followed by a strong impact from a falling sphere (D). A fishing knot is tightened (E). Eight scuzzy hairy balls are compressed and released (F). A house of cards collapses with a gentle touch by a rolling sphere (G). Ten sheets are smashed onto the ground by a fast falling heavy sphere (H). Peak contact counts are 168.35 million (A), 17.59 million (D), 6.49 million (C), 6.04 million (B), 5.53 million (H), 2.85 million (F). Average time per video frame is 194s (A), 245s (B), 247s (C), 144s (D), 3.30s (F), 196s (E), 5.04s (G), 77.35s (H).

This paper presents a new cubic barrier with elasticity-inclusive dynamic stiffness for penetration-free contact resolution and strain limiting. We show that our method enlarges tight strain-limiting gaps where logarithmic barriers struggle and enables highly scalable contact-rich simulation.

CCS Concepts • Computing methodologies • Physical simulation.

purely volumetric approaches ill-suited for codimensional colliders [Allard et al. 2010; Chen et al. 2023; Faure et al. 2008; Tang et al. 2012]. If collisions are unresolvable, one may resort to a rigid impact zone [Haraux et al. 2008; Hu et al. 2001; Proval 1997], rigidifying and delaying the collision resolution to the next step [Bridson et al.

Ingredients for basic shell simulation

- Input: Non-planar triangle mesh in 3D

- **In-plane stresses:** 2D elasticity

- Neo-Hookean: $\Psi_{\text{NH}} = \frac{\mu}{2}(\text{tr}(\mathbf{C}) - 2) - \mu \ln(J) + \frac{\lambda}{2} \ln(J)^2$
with $\mathbf{C} = \mathbf{F}^T \mathbf{F}$ and $J = \sqrt{\det(\mathbf{C})}$

- Deformation gradient: $\mathbf{F} \in \mathbb{R}^{3 \times 2}$ such that $\mathbf{j}^e = \mathbf{F} \mathbf{J}^e$
(maps vectors from 2D reference to 3D current configuration)

- Current configuration: $\mathbf{j}^e = [\mathbf{x}_1 - \mathbf{x}_0, \mathbf{x}_2 - \mathbf{x}_0]$

- For reference configuration, rotate triangle Ω^e into planar configuration:
(only edge lengths relevant, model Ψ_{NH} is rotationally invariant)

- Translate to origin: $\mathbf{u}_0 = [0, 0]^T$

- Align first edge with x-axis: $\mathbf{u}_1 = [\|\mathbf{X}_1 - \mathbf{X}_0\|, 0]^T$

- Rotate third vertex into x-y plane:

$$\mathbf{u}_{2,x} = (\mathbf{X}_1 - \mathbf{X}_0) \cdot (\mathbf{X}_2 - \mathbf{X}_0) \|\mathbf{X}_1 - \mathbf{X}_0\|^{-1}$$

$$\mathbf{u}_{2,y} = \sqrt{\|\mathbf{X}_2 - \mathbf{X}_0\|^2 - \mathbf{u}_{2,x}^2}$$

$$\mathbf{u}_2 = [\mathbf{u}_{2,x}, \mathbf{u}_{2,y}]^T$$

- Then: $\mathbf{J}^e = [\mathbf{u}_1 - \mathbf{u}_0, \mathbf{u}_2 - \mathbf{u}_0]$

Alternatively:



- **Strain limiting:** Singular Value Barriers [Li 2021]

- Compute singular values σ_1, σ_2 of $\mathbf{E} = \frac{1}{2}(\mathbf{C} - \mathbb{1})$

- Define barrier per singular value with strain limit s and barrier activation threshold \hat{s} :

$$b_{\text{SL},i}(\mathbf{x}) = \begin{cases} -\left(\frac{\hat{s} - \sigma_i}{s - \hat{s}}\right)^2 \ln\left(\frac{s - \sigma_i}{s - \hat{s}}\right), & \sigma_i > \hat{s} \\ 0 & \sigma_i \leq \hat{s} \end{cases}$$

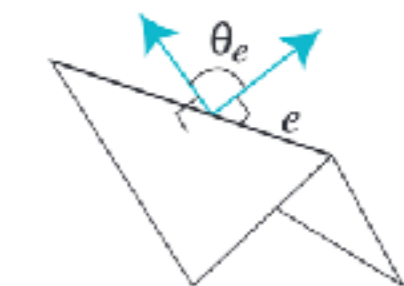
- Integrate over element volume:

$$\phi_{\text{SL}}^e = \kappa_{\text{SL}} \sum_i \int_{\Omega^e} b_{\text{SL},i}(\mathbf{x}) d\mathbf{X} \approx \kappa_{\text{SL}} V^e \sum_i b_{\text{SL},i}$$

- **Out of plane bending:** Discrete Shells [Grinspun 2003] or Quadratic Bending [Bergou 2006]

- Potential per interior edge, depends on dihedral angle:

$$\phi_{\text{B}}(\mathbf{x}) = \kappa_{\text{B}} \frac{\|\mathbf{e}_0\|}{h_0} (\theta(\mathbf{x}) - \theta_0)^2$$



- For rest-flat shells a quadratic formulation in vertex positions exists (constant Hessian)

Rigid Bodies & Affine Bodies

- DOF per rigid body: translation $\mathbf{x}_i \in \mathbb{R}^3$ and rotation vector $\boldsymbol{\theta}_i \in \mathbb{R}^3$

- Inertial term for rotation DOF:

$$E_R(\mathbf{R}(\boldsymbol{\theta})) = \sum_i^{N_{rb}} \left(\frac{1}{2} \text{tr}(\mathbf{R}_i \mathbf{J}_i \mathbf{R}_i^T) - \text{tr}(\mathbf{R}_i \mathbf{J}_i \tilde{\mathbf{R}}_i^T) \right)$$

with $\tilde{\mathbf{R}}_i = \mathbf{R}_i^{\text{prev}} + h \dot{\mathbf{R}}_i^{\text{prev}} + h^2 \tau_i \mathbf{J}_i^{-1}$

- Non-linear mapping from DOF to vertices
 - Small time steps or “curved CCD” for intersection-free contact

- Alternative: **Affine Bodies**

- Body embedded in a single tetrahedron
- Use any stiff material model ($E > 10^8 \text{Pa}$)

Intersection-free Rigid Body Dynamics

ZACHARY FERGUSON, New York University
 MINCHEN LI, University of California, Los Angeles and University of Pennsylvania
 TESEO SCHNEIDER, New York University and University of Victoria
 FRANCISCA GIL-LURETA, New York University
 TIMOTHY LANGLOIS, Adobe Research
 CHENFANFU JIANG, University of California, Los Angeles and University of Pennsylvania
 DENIS ZORIN, New York University
 DANNY M. KAUFMAN, Adobe Research
 DANIELE PANOZZO, New York University


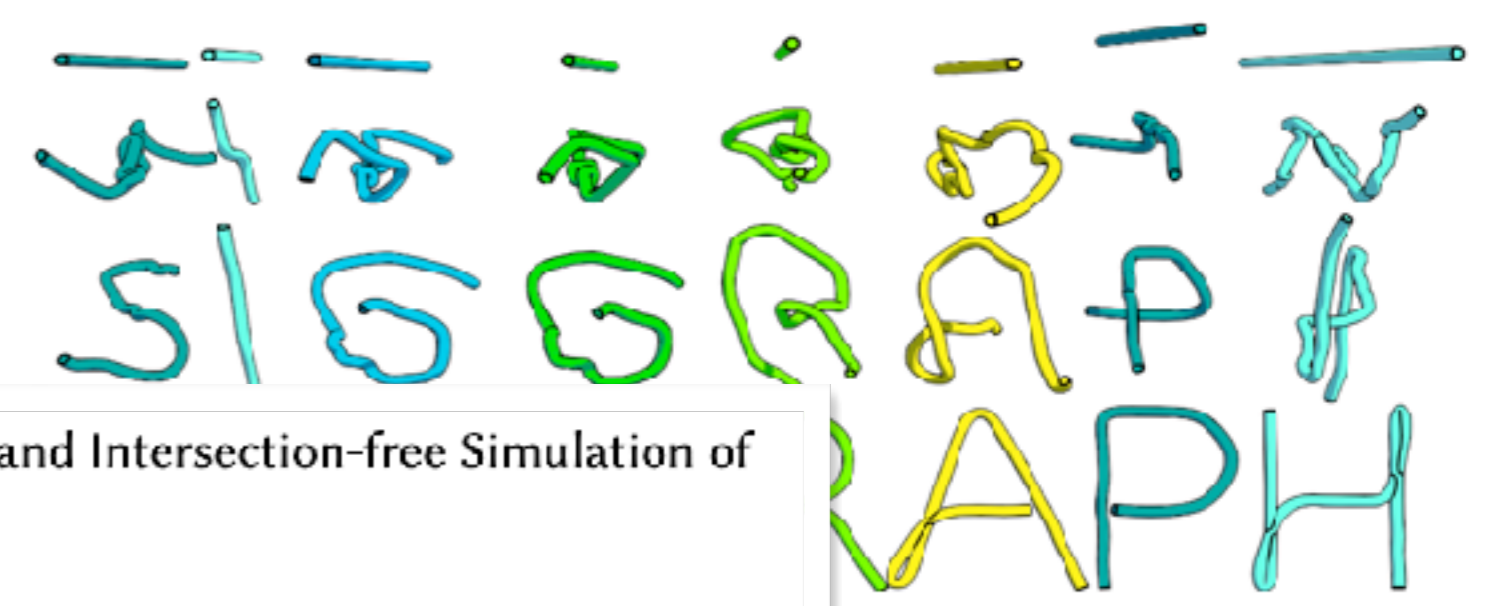


Fig. 1. Expanding Lock Box. An intricate locking mechanism with a central spiral is rotated which in turn pulls in each of the... intersection-free guarantee enables the automatic test...

Painless Differentiable Rotation Dynamics

MAGÍ ROMANYÀ-SERRASOLSAS, Universidad Rey Juan Carlos, Spain
 JUAN J. CASAFRANCA, Universidad Rey Juan Carlos, Spain
 MIGUEL A. OTADUY, Universidad Rey Juan Carlos, Spain



simulation frames they spell "SIGGRAPH". Our approach based on Lie... rotation vectors.

Introduction
well known that the nonlinear nature of the space of rotations... into integrals contributes to the non-linear nature of the simulation.

Affine Body Dynamics: Fast, Stable and Intersection-free Simulation of Stiff Materials

LEI LAN, Clemson University & University of Utah, USA
 DANNY M. KAUFMAN, Adobe Research, USA
 MINCHEN LI, University of California, Los Angeles & TimeStep Inc., USA
 CHENFANFU JIANG, University of California, Los Angeles & TimeStep Inc., USA
 YIN YANG, Clemson University, University of Utah & TimeStep Inc., USA

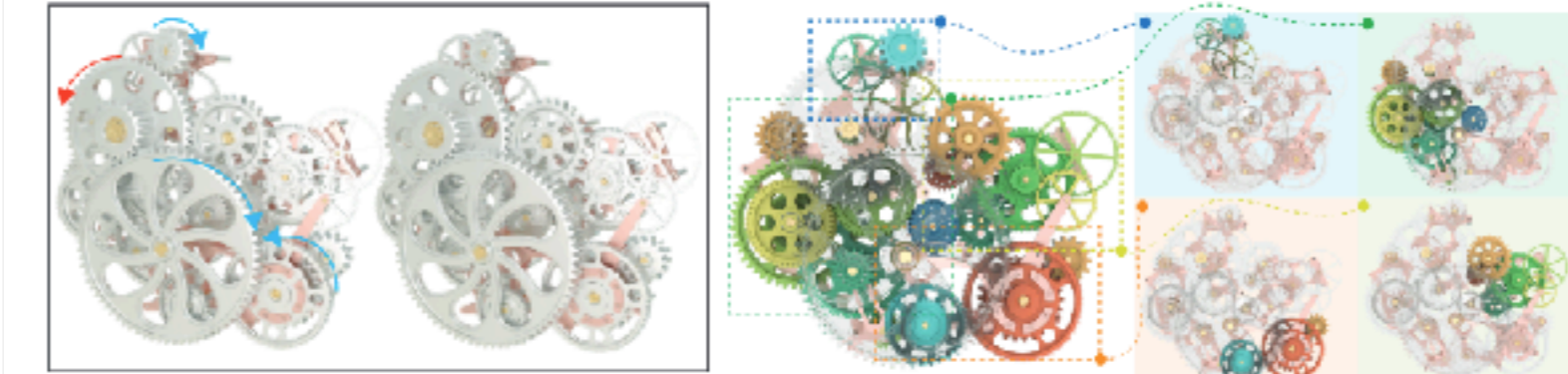


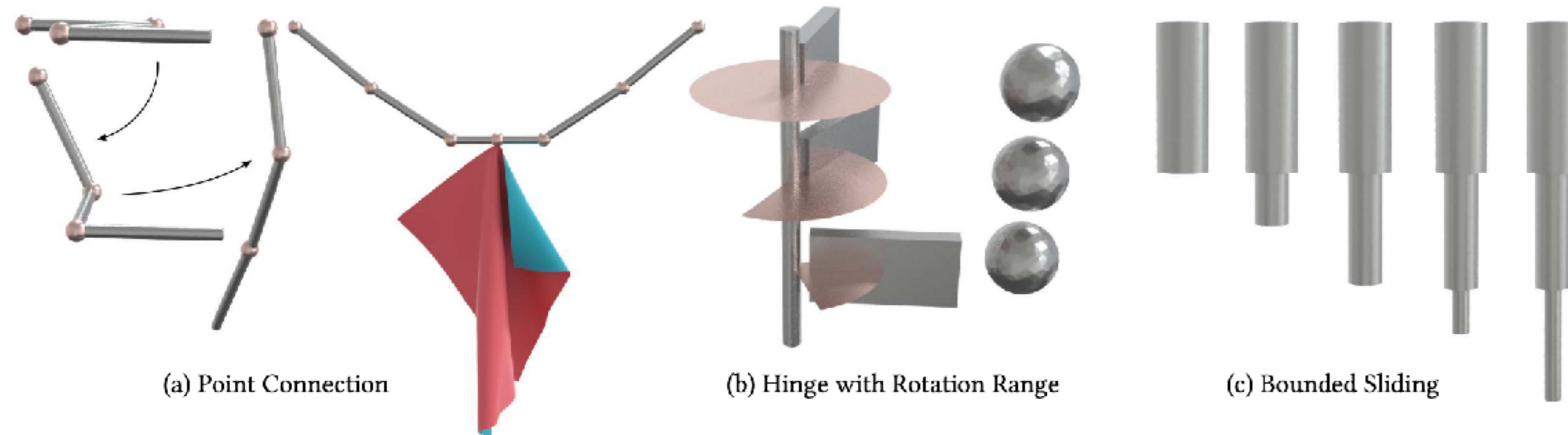
Fig. 1. Geared system. We propose an affine body dynamics (ABD) framework to efficiently and robustly simulate close-to-rigid contacting objects. ABD... collision and contact processing costs over rigid body modeling while obtaining high-quality, intersection-free trajectories leveraging barrier-based... frictional contact modeling. In this challenging stress-test benchmark we simulate a complex geared system composed of 28 toothed gears with frictional... contact resolving all interactions. The combined gear set mesh is comprised of over 2.5M surface triangles. A torque applied to the actuated gear (red arrow)... drives the motion of the entire system via contact, with over a quarter of all surface elements in active contact in every time step. Here we find that all... existing rigid body simulation algorithms, including rigid MPC, fail to make progress, while ABD robustly simulates the example to completion. ABD enables large... time step sizes (e.g., with $\Delta t = 1/50$ sec) even for such challenging, large displacement (rotation) contact processing. For a time step size of 1/100 sec, ABD... simulates each step in less than 12 sec on an Intel i7 CPU (multi-threaded), while the simulation runs interatively on a 3600 CPU (5-10 steps per second).

Multi-Body Systems

- Coupling deformable & rigid bodies with joints and motors
- Reformulate constraints using penalties and barriers

→ Equality constraints: $\phi_{\text{Eq}}(\mathbf{x}) = \frac{1}{2}k(c(\mathbf{x}))^2$

→ Inequality constraints: $\phi_{\text{Ineq}}(\mathbf{x}) = \kappa b(c(\mathbf{x}))$



A Unified Newton Barrier Method for Multibody Dynamics

YUNUO CHEN*, University of California, Los Angeles, USA
MINCHEN LI*, University of California, Los Angeles & TimeStep Inc., USA
LEI LAN, Clemson University & University of Utah, USA
HAO SU, University of California, San Diego, USA
YIN YANG, Clemson University, University of Utah & TimeStep Inc., USA
CHENFANFU JIANG, University of California, Los Angeles & TimeStep Inc., USA

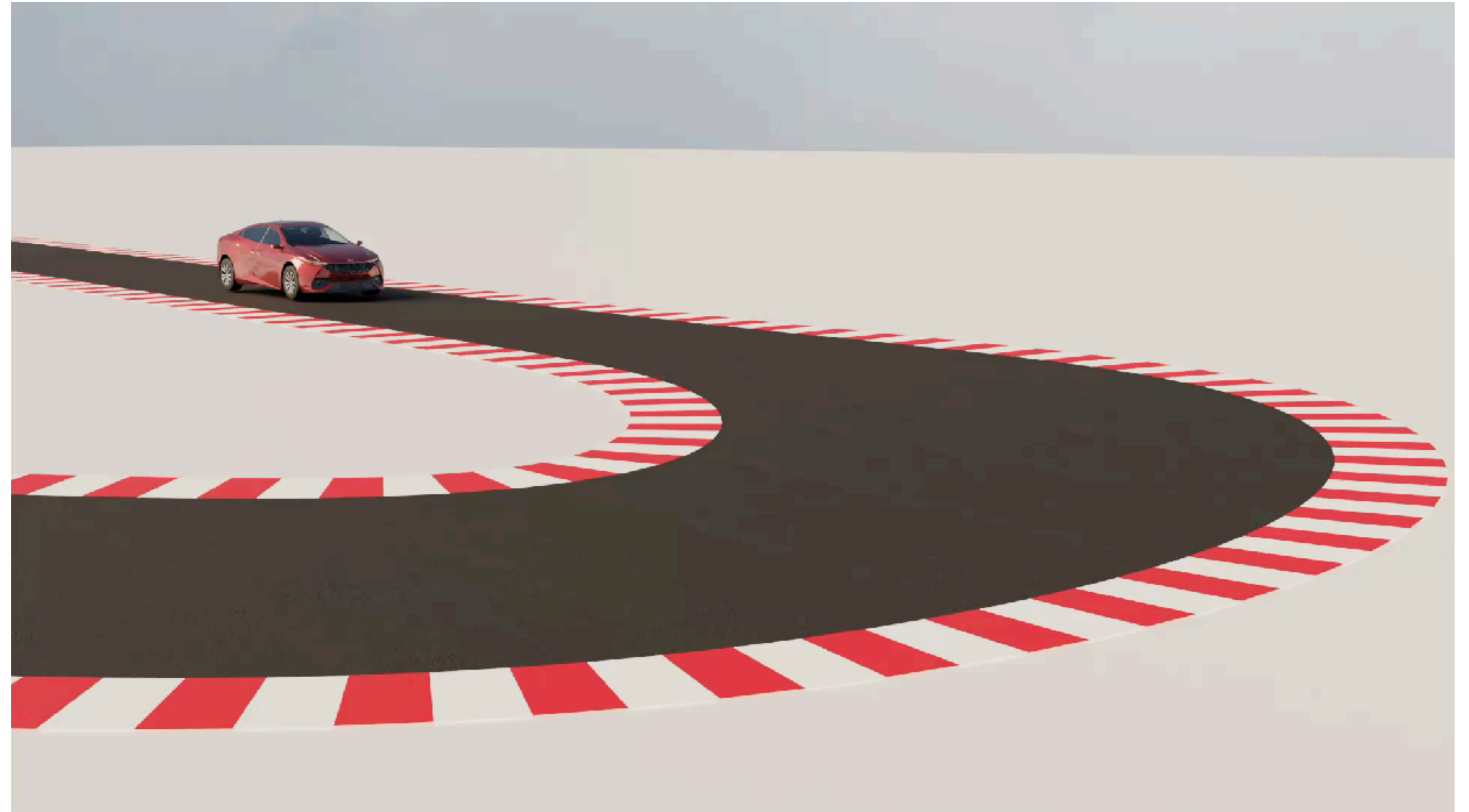


Fig. 1. "Lying Flat". Our primal Newton Barrier Method provides a unified simulation framework for this complex multibody system, consisting of a hammock made with rigid (stiff) rings, neo-Hookean deformable tori and circular rods, as well as an eleven-part articulated ragdoll and a piece of cloth. Accurate resolutions of the frictional contact and articulation constraints are guaranteed robustly, stably, and efficiently.

Multi-Body Systems

Strongly coupled systems:

- Rigid bodies for car body and rims
- Tires as deformable solids
- Dampened springs and slider joints for suspension
- Connected with axial joints
- Rotation limits for steering

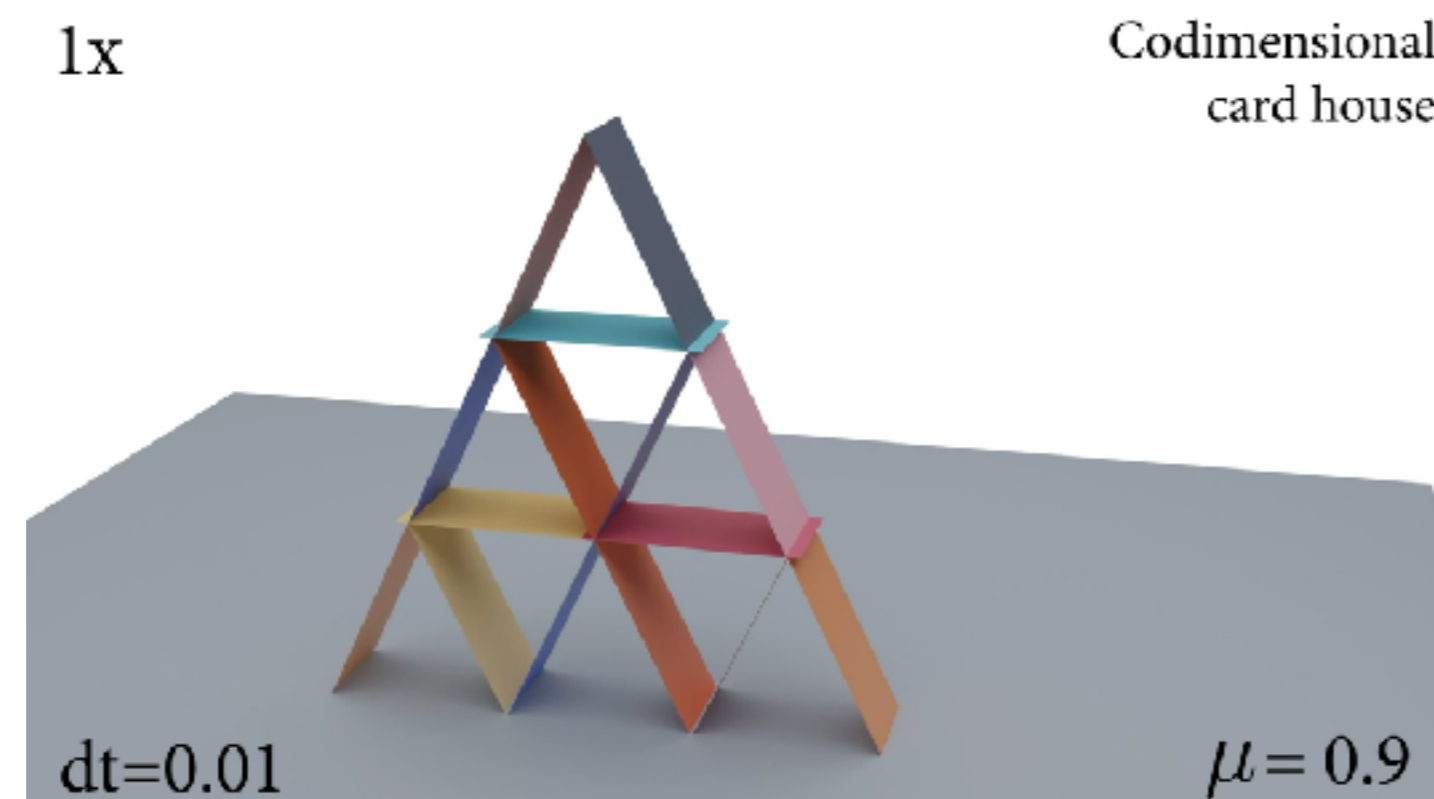


SymX: Energy-based Simulation from Symbolic Expressions [Fernández-Fernández et al. 2025]

Dissipative Forces

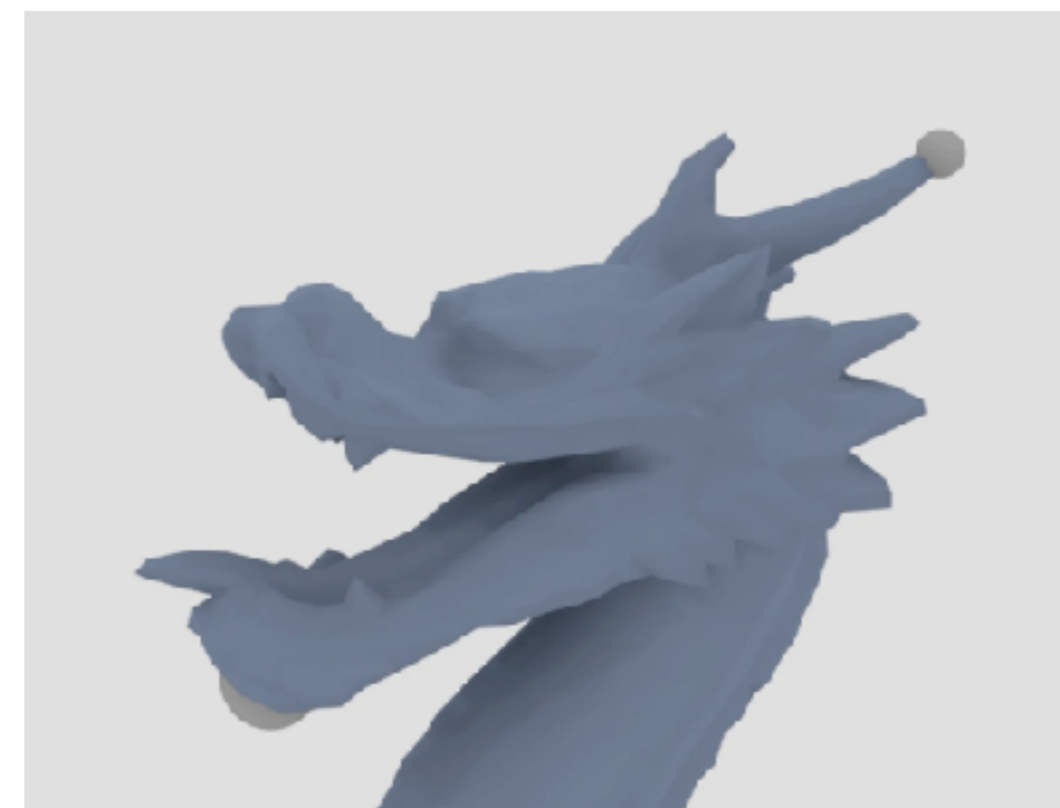
- We need scalar potentials $\phi_i(\mathbf{x})$ such that $\mathbf{f}_i(\mathbf{x}) = -\nabla \phi_i(\mathbf{x})$
 - Possible for conservative and path-independent forces
- Adaptations required for dissipative/non-conservative forces:

Friction



Intersection-free Rigid Body Dynamics [Ferguson et al. 2021]

Damping



Accurate Dissipative Forces in Optimization Integrators [Brown et al. 2018]

Plasticity



Energetically Consistent Inelasticity for Optimization Time Integration [Li et al. 2020]

Damping

- Common damping & friction forces can be written as **dissipation potential**

$$R(\mathbf{x}, \mathbf{v}) \text{ s.t. } \mathbf{f}_d = -\nabla_{\mathbf{v}} R(\mathbf{x}, \mathbf{v})$$

- Not generally possible to define potential $\phi_d(\mathbf{x})$ s.t. $-\nabla_{\mathbf{x}} \phi_d = \mathbf{f}_d$

- Example: **Rayleigh damping**

- Forces: $\mathbf{f}_d = -(\alpha \mathbf{M} + \beta \mathbf{K}(\mathbf{x})) \mathbf{v}$

- Dissipation potential: $R_{\text{ray}}(\mathbf{x}, \mathbf{v}) = \frac{1}{2} \mathbf{v}^T (\alpha \mathbf{M} + \beta \mathbf{K}(\mathbf{x})) \mathbf{v}$

- Approximation by lagging: $\mathbf{K}(\mathbf{x}) \approx \mathbf{K}(\mathbf{x}^{\text{prev}})$

- Lagged potential: $\phi_{\text{ray}}(\mathbf{x}) = \frac{1}{2\Delta t} (\mathbf{x} - \mathbf{x}^{\text{prev}})^T (\alpha \mathbf{M} + \beta \mathbf{K}(\mathbf{x}^{\text{prev}})) (\mathbf{x} - \mathbf{x}^{\text{prev}})$

Accurate Dissipative Forces in Optimization Integrators

GEORGE E. BROWN, University of Minnesota
 MATTHEW OVERBY, University of Minnesota
 ZAHRA FOROOTANINIA, University of Minnesota
 RAHUL NARAIN, Indian Institute of Technology

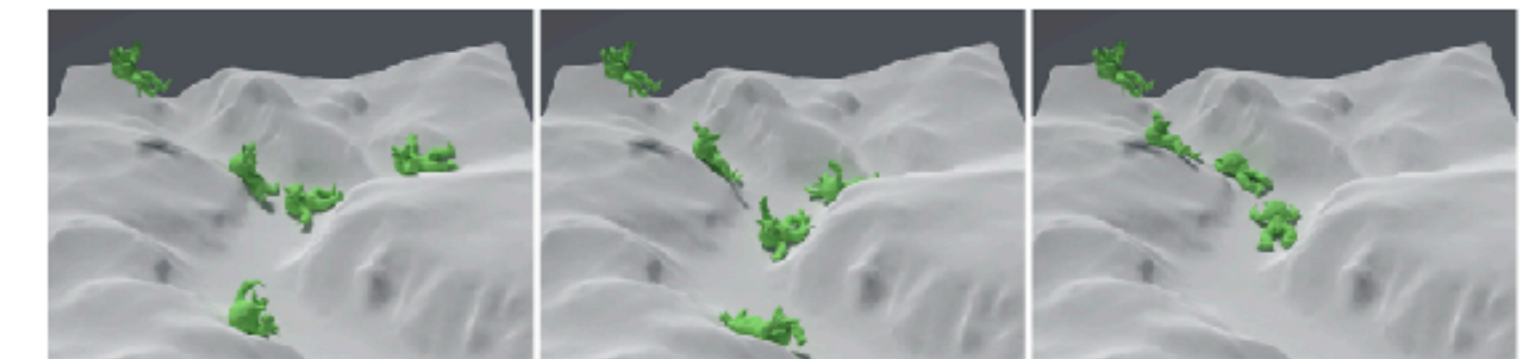


Fig. 1. A Neo-Hookean armadillo falls down a complex terrain with different friction coefficients, left: $\mu = 0$, center: $\mu = 0.15$, right: $\mu = 0.45$.

We propose a method for accurately simulating dissipative forces in deformable bodies when using optimization-based integrators. We represent such forces using *dissipation functions* which may be nonlinear in both positions and velocities, enabling us to model a range of dissipative effects including Coulomb friction, Rayleigh damping, and viscoplasticity.

In animation applications, there is also an ever-increasing need to extend the complexity of simulations that can be carried out in a fast and stable manner. However, achieving both speed and stability when modeling nonlinear phenomena is a challenging

TRANSACTIONS ON VISUALIZATION AND COMPUTER GRAPHICS

Optimization Integrator for Large Time Steps

Theodore F. Gast, Craig Schroeder, Alexey Stomakhin, Chentantu Jiang and Joseph M. Teran

Abstract—Practical time steps in today's state-of-the-art simulators typically rely on Newton's method to solve large systems of nonlinear equations. In practice, this works well for small time steps but is unreliable at large time steps at or near the frame rate, particularly for difficult or stiff simulations. We show that recasting backward Euler as a minimization problem allows Newton's method to be stabilized by standard optimization techniques with some novel improvements of our own. The resulting solver is capable of solving even the toughest simulations at the 24 Hz frame rate and beyond. We show how simple collisions can be incorporated directly into the solver through constrained minimization without sacrificing efficiency. We also present novel penalty collision formulations for self collisions and collisions against scripted bodies designed for the unique demands of this solver. Finally, we show that these techniques improve the behavior of Material Point Method (MPM) simulations by recasting it as an optimization problem.

Index Terms—Computer Graphics, Three-Dimensional Graphics and Realism, Animation

1 INTRODUCTION

THE most commonly used time integration schemes in use today for graphics applications are implicit methods. Among these, backward Euler [1], [2], [3], [4], [5] or variants on Newmark methods [5], [7], [8] are the most common, though even more sophisticated schemes like BDF-2 [9], [10], implicit-explicit

constraints robustly and efficiently [2] shows that supplementing Newton's method with a line search greatly improves robustness. [4] also shows that supplementing Newton's method with a line search and a definiteness correction leads to a robust solution procedure. Following their example, we show that recasting the

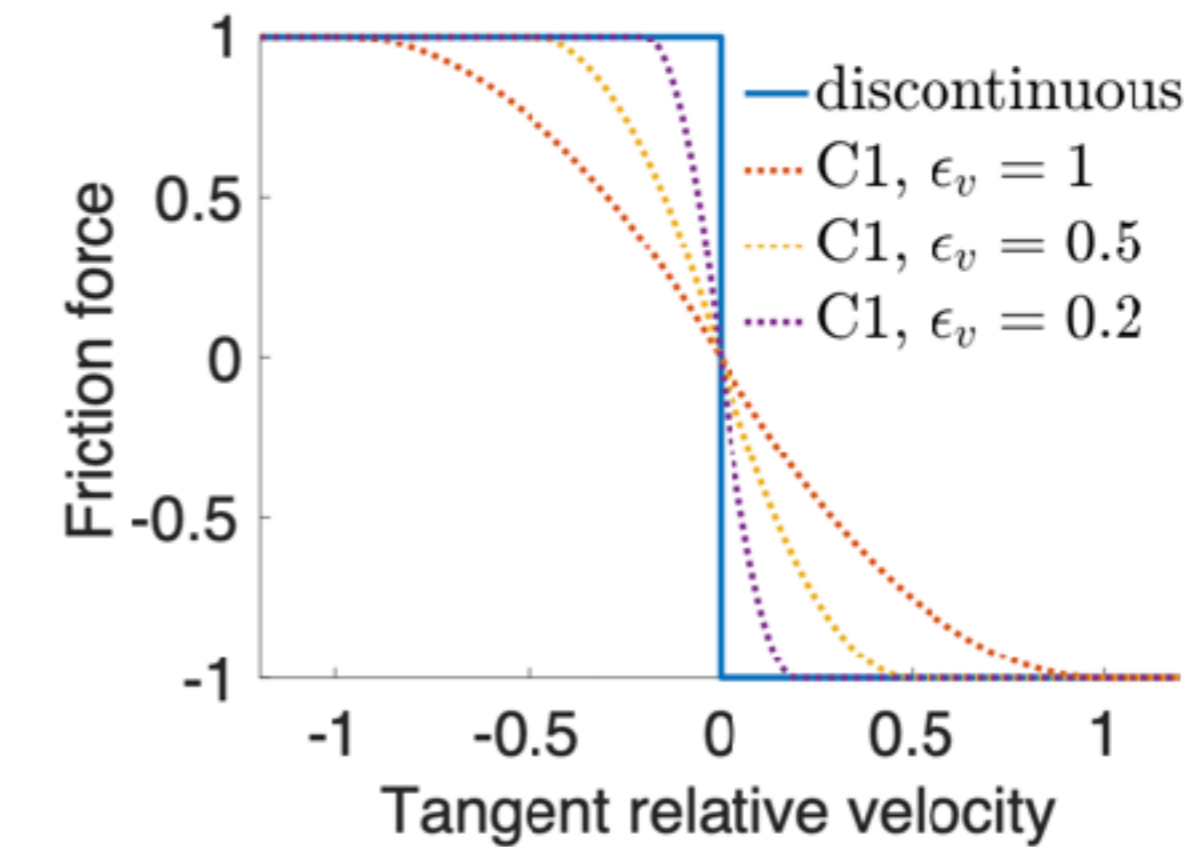
Friction

- Example: **Coulomb friction**

- Again, can be formulated as dissipation potential $R(\mathbf{x}, \mathbf{v})$ s.t. $\mathbf{f}_f = -\nabla_{\mathbf{v}}R(\mathbf{x}, \mathbf{v})$
- But not as energy potential without approximation
- Also: Non-smoothness at **stick-slip transition**

- Solution of [Li et al. 2020]:

- C^1 -smooth transition between static and dynamic friction with velocity threshold ϵ_v
- Lagging of tangential sliding basis and contact force magnitude
- Only relative sliding displacement \mathbf{x} is fully implicit
- Can lead to inaccurate behavior in friction sensitive problems

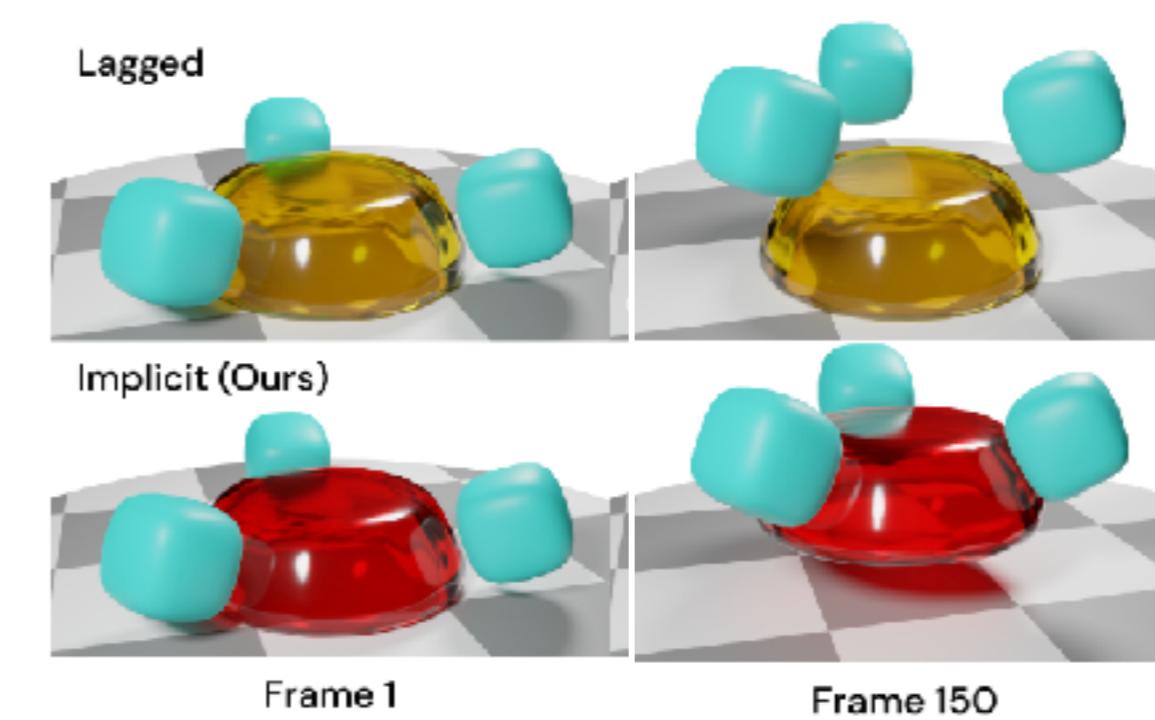


Incremental Potential Contact [Li et al. 2020]

Incremental Potential Contact: Intersection- and Inversion-free, Large-Deformation Dynamics

MINCHEN LI, University of Pennsylvania & Adobe Research
 ZACHARY FERGUSON and TESEO SCHNEIDER, New York University
 TIMOTHY LANGLOIS, Adobe Research
 DENIS ZORIN and DANIELE PANOZZO, New York University
 CHENFANFU JIANG, University of Pennsylvania
 DANNY M. KAUFMAN, Adobe Research

Fig. 1. Sparse multi-incremental Potential Contact (PC) enables high-rate time stepping, here with $\Delta t = 0.01s$, of extreme nonlinear elastodynamics with contact that is intersection- and inversion-free at all time steps, irrespective of the degree of compression and contact. Here a plate compresses and then forces a collection of complex soft elastic FE models (BIBS tetrahedra in total, with a neo-Hookean material) through a thin, 3D-printed elastica tube. The models are then compressed elastically together forming a tight mesh to fit through the gap and then once they decouple they stably separate into a stable pile.



Implicit frictional dynamics with soft constraints [Larionov et al. 2024]

Implicit frictional dynamics with soft constraints

Egor Larionov, Andreas Lougva, Uri M. Ascher, Jan Bender, and Daniele P. K. Pai

Abstract—Dynamics simulation with frictional contacts is important for a wide range of applications, from cloth simulation to object manipulation. Recent methods using smoothed lagged friction forces have enabled robust and differentiable simulation of elastodynamics with friction. However, the resulting frictional behavior can be inaccurate and may not converge to analytic solutions. Here we evaluate the accuracy of lagged friction models in comparison with implicit frictional contact systems. We show that major inaccuracies near the stick-slip threshold in such systems are caused by lagging of friction forces rather than by smoothing the Coulomb friction curve. Furthermore, we demonstrate how systems involving implicit or lagged friction can be correctly used with higher-order time integration and highlight limitations in earlier attempts. We demonstrate how to exploit forward-mode automatic differentiation to simplify and, in some cases, improve the performance of the exact Newton method. Finally, we show that often complex phenomena can also be simulated effectively while maintaining smoothness of the entire system. We extend our method to exhibit stick-slip frictional behavior and preserve volume in compressible and nearly-incompressible media using soft constraints.

Index Terms—dry friction, contact, elasticity, deformable object dynamics

forces implicitly when computing friction, our method can produce more accurate friction behavior, and it requires no additional iterations or specialized mechanisms for computing friction, contact and elasticity.

Frictional contact is traditionally modeled as a non-smooth problem requiring sophisticated tools. In particular, non-smooth integrators, root finding or optimization techniques are needed for handling inclusion terms in the mathematical model. This drastically complicates the problem and substantially limits the number of solution approaches. While non-smoothness is required to guarantee absolute sticking, it is not generally necessary if simulations are limited in time. In fact, when observed on a microscale, even dry friction responds continuously to changes in velocity [3]. Accordingly, we adopt a smooth friction formulation. We show that when applied fully implicitly in the equations of motion, it can produce predictable sticking. In contrast, our study shows that the popular approach of lagging friction causes inaccurate and time-step dependent sticking behavior. In particular, we demonstrate the importance of evaluating the sliding basis

Coupling Magnetic Effects

Magnetic Rigid Bodies



Strongly Coupled Simulation of Magnetic Rigid Bodies [Westhofen et al. 2024]

$$\phi_{\text{magn}} = - \sum_i V_i \mathbf{M}_i \cdot \mathbf{B}_{\text{ext},i}$$

Magnetoelastic Thin Shells



Simulation and Optimization of Magnetoelastic Thin Shells [Chen et al. 2022]

$$\phi_{\text{magn}} = - \sum_i h \mathbf{F}_i \mathbf{M}_i \cdot \mathbf{B}_{\text{ext},i}$$

FEM & SPH Coupling: Contact Proxy Splitting Method

- Fully Lagrangian formulation
- Models **Weakly Compressible SPH** using quadratic potentials

- e.g. incompressibility potential: $\phi_{\text{Inc}} = \sum_i \frac{\kappa_I}{2} V_0 \left(\frac{\rho_0}{\rho_i} - 1 \right)^2$

- Contact model: barriers on particle \leftrightarrow mesh distances

Problems of fully implicit formulation:

- “Connectivity” of SPH particles (neighbors of neighbors)
- Nonlinearity of barriers and deformables

Splitting approach:

1. Solve **fluid** phase with **linearized contact** forces
2. Solve **deformables** with **full contact** potential & **fluid proxy**

A Contact Proxy Splitting Method for Lagrangian Solid-Fluid Coupling

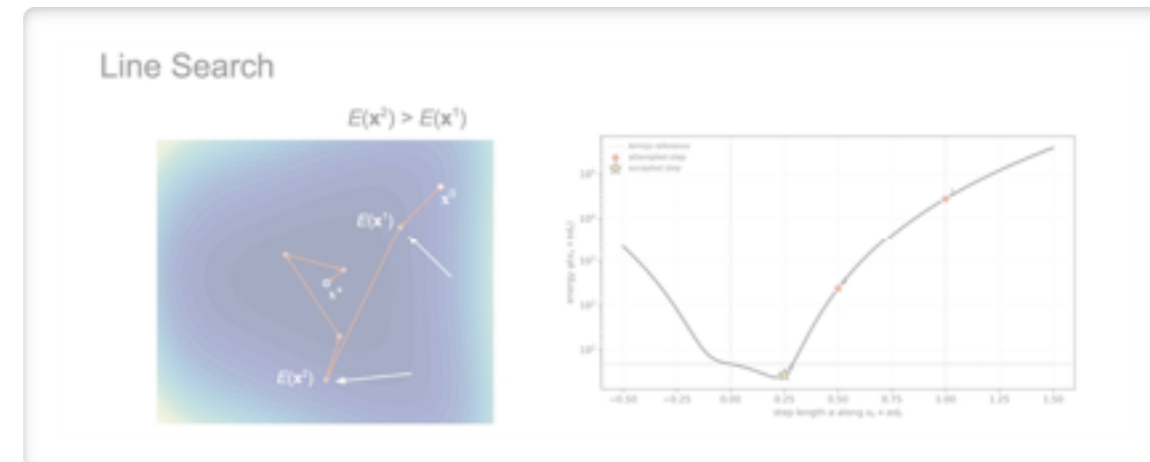
TIANYI XIE, University of California, Los Angeles, USA
MINCHEN LI, University of California, Los Angeles, USA
YIN YANG, University of Utah, USA
CHENFANFU JIANG, University of California, Los Angeles, USA



Fig. 1. Kick water. Our method accurately captures the complex interactions between the water, the multi layer skirt, and the mannequin body without any interpenetration as the mannequin wearing the skirt kicks in a swimming pool and sends water flying.



Outline



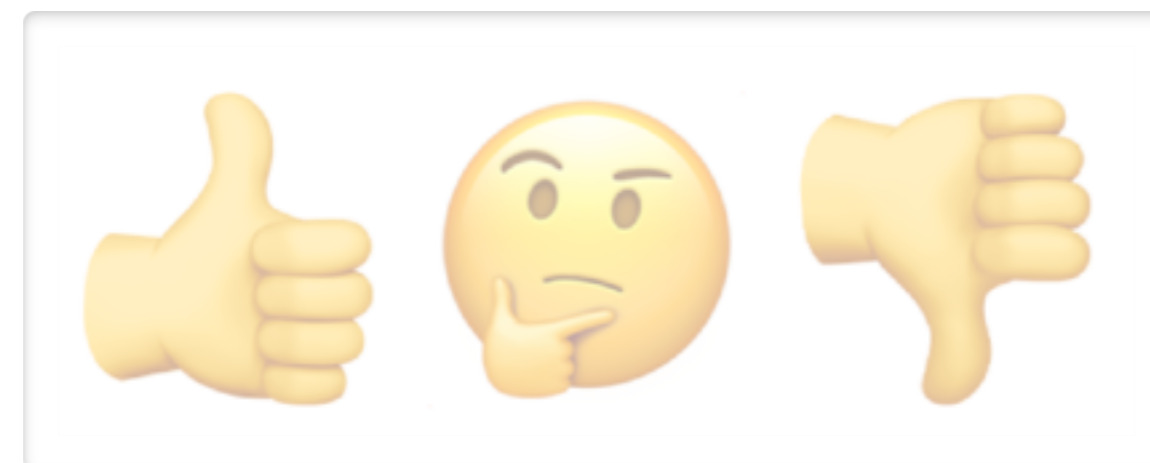
1. Mathematical foundations



2. Physical models and coupling



3. Related methods (VBD, PD)



4. Summary: Models & Properties

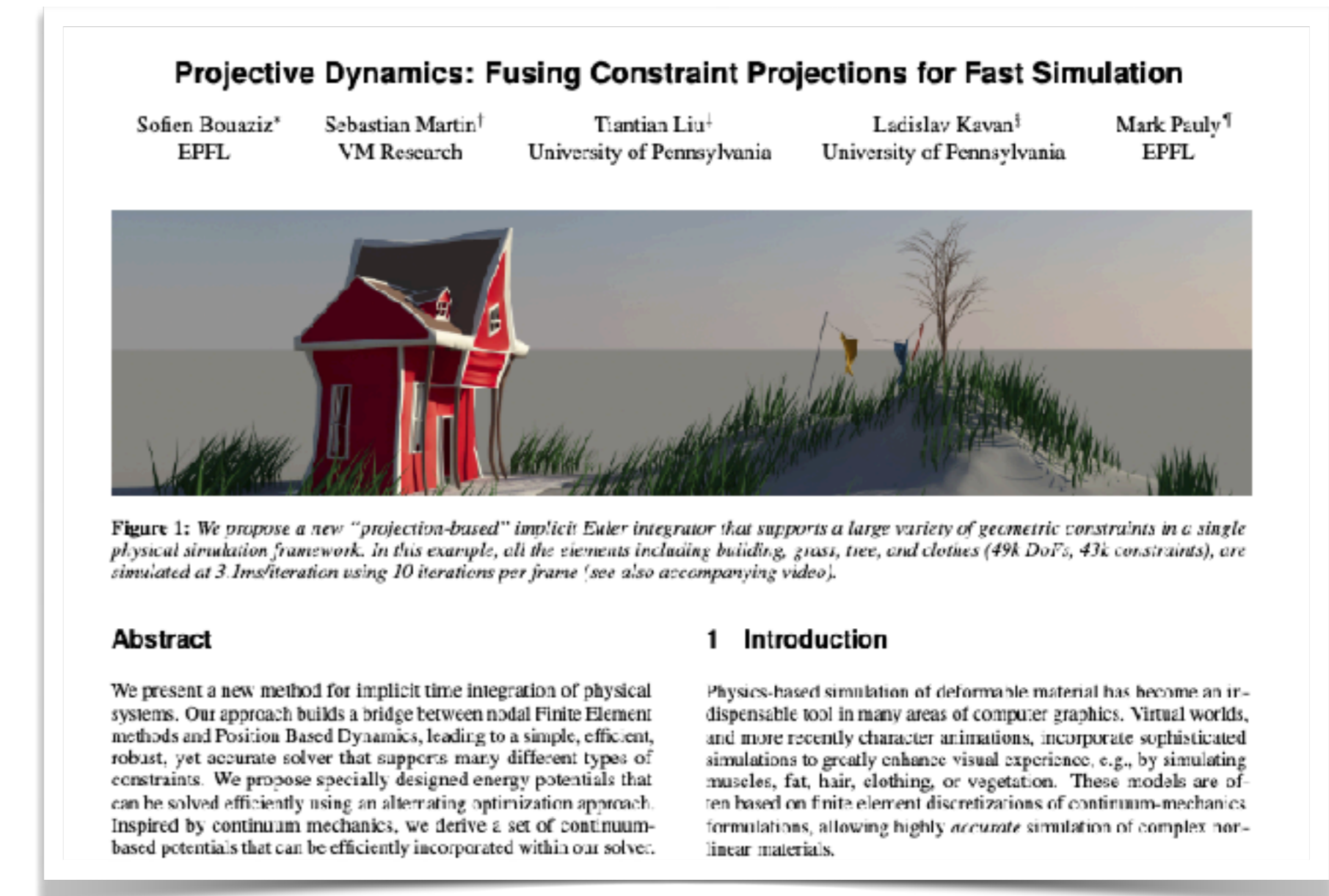
Projective Dynamics

- Introduces local/global split
- **Local:** Non-linear constraint projections
 - **Per constraint**, find closest “target positions” \mathbf{p}_i that satisfy $\mathbf{C}_i(\mathbf{p}_i) = 0$
- **Global:** for fixed \mathbf{p}_i , minimize BE incremental potential

$$E_{\text{PD}}(\mathbf{x}, \mathbf{p}) = \frac{1}{2\Delta t^2}(\mathbf{x} - \tilde{\mathbf{x}})^\top \mathbf{M}(\mathbf{x} - \tilde{\mathbf{x}}) + \sum_i d_i(\mathbf{x}, \mathbf{p}_i)$$

→ Where $d_i(\mathbf{x}, \mathbf{p}_i)$ are **quadratic** functions, pulling the DOF \mathbf{x} towards \mathbf{p}_i

E_{PD} has Constant Hessian → Pre-Factorize



Projective Dynamics

- Geometrically motivated models for deformables, shells, rods
- Constraints for strain limiting, joints and contacts
- Generalizations with ADMM and as Quasi-Newton method
- Compared to XPBD: better convergence properties but less general

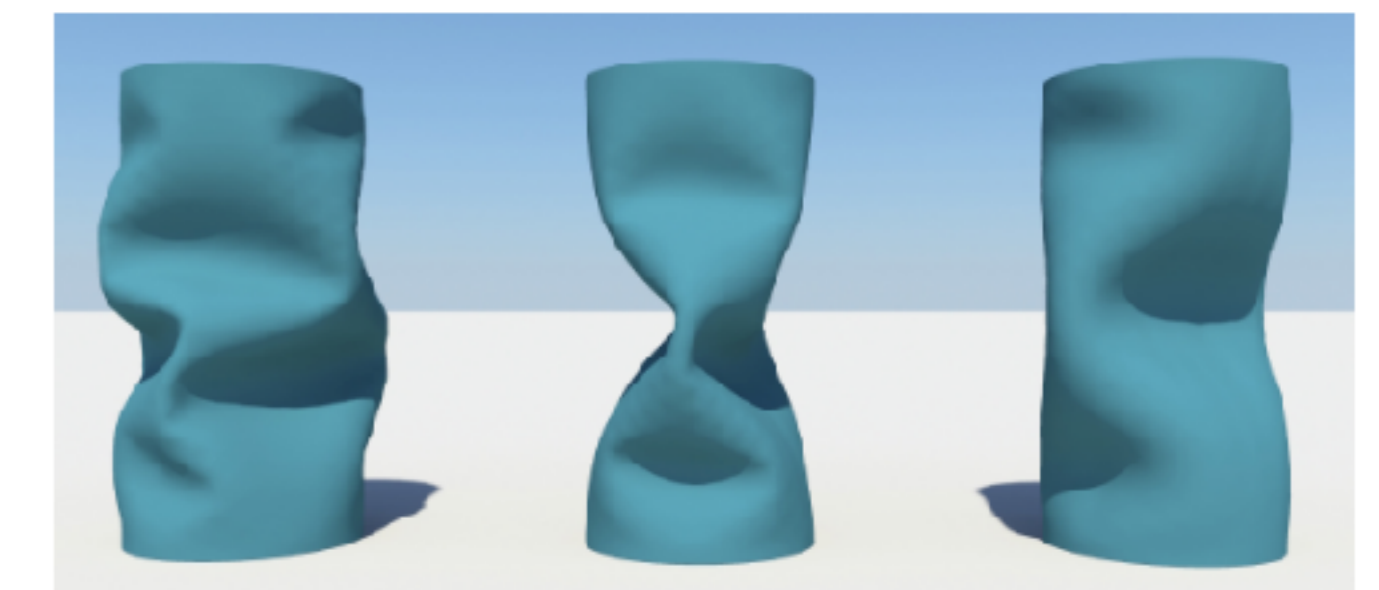


Penetration-free Projective Dynamics on the GPU [Lan et al. 2022]

Example-based materials



Thin shells



[Bouaziz et al. 2014]

Vertex Block Descent

- Uses a block coordinate descent approach
- Solves **local** (per-vertex) energies:

$$E_i(\mathbf{x}) = \frac{m_i}{2\Delta t^2} \|\mathbf{x}_i - \tilde{\mathbf{x}}_i\|^2 + \sum_{j \in \mathcal{V}_i} \phi_j(\mathbf{x})$$

Energies affecting vertex i

- Analytic inversion of local **3x3 Hessians**
- Designed for efficient implementation on GPU
- Alternative to XPBD, but is a **primal** method
- Reduces global energy but does not necessarily converge to its minimum

Vertex Block Descent

ANKA HE CHEN, University of Utah, USA
 ZIHENG LIU, University of Utah, USA
 YIN YANG, University of Utah, USA
 CEM YUKSEL, University of Utah, USA and Roblox, USA




Fig. 1. Example simulation results using our solver, both of these methods involve more than 100 million DoFs and 1 million active collisions.

We introduce vertex block descent, a block coordinate descent solution for the variational form of implicit Euler through vertex level Gauss Seidel iterations. It operates with local vertex iterations in global variational energy with

1 INTRODUCTION
 Physics-based simulation is the cornerstone of most graphics an-

Augmented Vertex Block Descent

CHRIS GILES, Roblox, USA
 ELIE DIAZ, University of Utah, USA
 CEM YUKSEL, University of Utah, USA

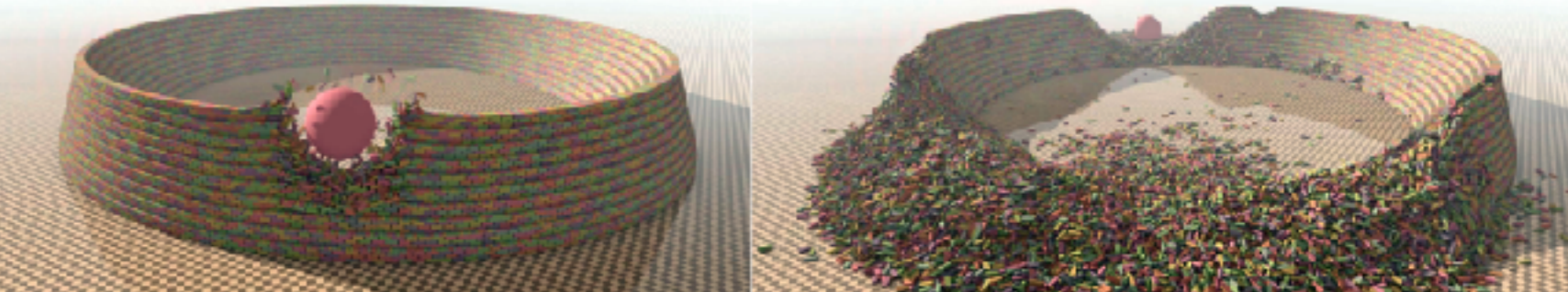
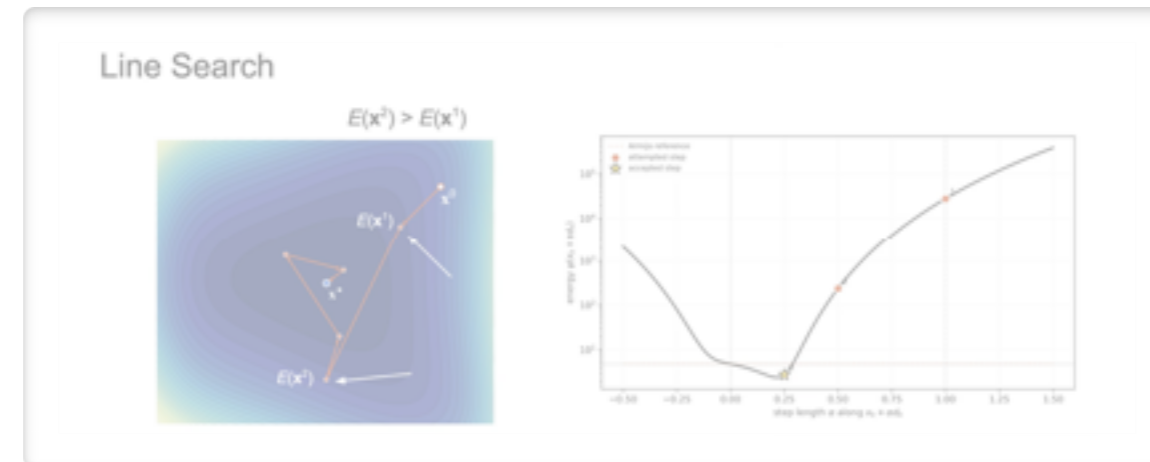


Fig. 1. Our augmented vertex block descent method allows simulating hard constraints, which are critical for handling contacts and stacking, shown here simulating a pile of 110,000 blocks smashed by a sphere using 4 iterations, taking 3.5 ms (9.8 ms including collision detection) per frame on an NVIDIA RTX 4050 GPU.

Vertex Block Descent is a fast physics-based simulation method that is unconditionally stable, highly parallelizable, and capable of converging to the implicit Euler solution. We extend it using an augmented Lagrangian formulation to address some of its fundamental limitations. First, we introduce a mechanism to handle hard constraints with infinite stiffness without

convergence behavior over prior techniques for soft body dynamics, delivering higher performance, improved parallelism, unconditional stability, and the ability to converge to the implicit Euler solution with the desired accuracy. In addition, VBD was shown to handle other simulation problems, such as particle systems and rigid body

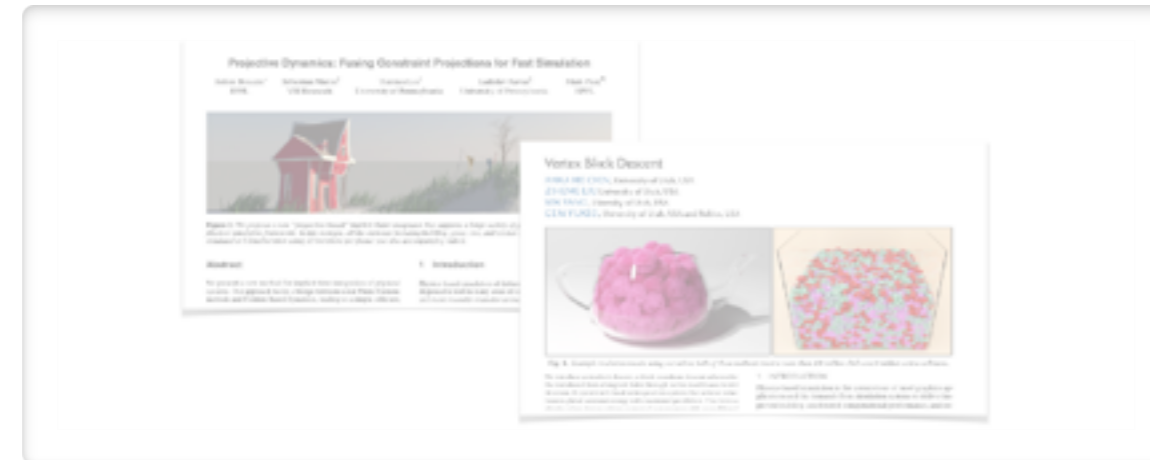
Outline



1. Mathematical foundations



2. Physical models and coupling



3. Related methods (VBD, PD)



4. Summary: Models & Properties

Summary: Energy-based Models

🌟 Deformable solids, cloth, shells and rods

👍 Geometrically motivated & continuum-based models

👍 Material models: isotropic, anisotropic, example-based, data-driven...

👍 Dynamic frictional contact & intersection-free simulations

👍 Rigid bodies & multi-body systems

👍 Other physical phenomena (e.g. magnetics, heating, wetting...)

🤔 “Accurate” friction and certain plasticity models

→ Typically needs approximations (e.g. lagging)

🤔 Fluids & granular media

→ Typically needs operator splitting, semi-implicit approaches or constrained optimization

Summary: Properties of Energy-Based Simulation

👍 **Simple:** in terms of formulation and numerical approach

👍 **Robust convergence:** due to line search & second-order derivatives

🤔 **Primal methods:** Good for high mass ratios, very large stiffness ratios numerically challenging

👎 **Limited to potentials:** no arbitrary dissipative and non-conservative forces

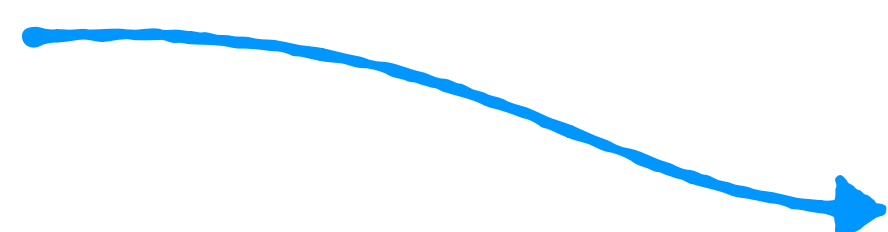
👉 Solution: Adapted and approximate models (for friction, damping and plasticity)

👎 **High computational cost:** problematic for interactive applications

👉 Alternative: Related methods for interactive applications, e.g.:

- VBD: Vertex Block Descent [Chen et al. 2024]
- PD: Projective Dynamics [Bouaziz et al. 2014]

} **Trade-offs in terms of convergence and/or generality**


$$f(\mathbf{x}) = -\nabla_{\mathbf{x}}\phi(\mathbf{x})$$

or

$$f_D(\mathbf{v}) = -\nabla_{\mathbf{v}}\phi_D(\mathbf{v})$$